

## **Oskarshamn site investigation**

### **Fracture mineralogy**

#### **Results from drill core KSH03A+B**

Henrik Drake

Department of Geology, Earth Sciences Centre  
Göteborg University

Eva-Lena Tullborg, Terralogica AB

January 2006

**Svensk Kärnbränslehantering AB**

Swedish Nuclear Fuel  
and Waste Management Co  
Box 5864

SE-102 40 Stockholm Sweden

Tel 08-459 84 00

+46 8 459 84 00

Fax 08-661 57 19

+46 8 661 57 19



# **Oskarshamn site investigation**

## **Fracture mineralogy**

### **Results from drill core KSH03A+B**

Henrik Drake

Department of Geology, Earth Sciences Centre

Göteborg University

Eva-Lena Tullborg, Terralogica AB

January 2006

*Keywords:* Fracture minerals, Simpevarp, formation temperatures, ductile/brittle deformation, relative dating, wall rock alteration, red-ox, low-temperature minerals, calcite, stable isotopes, sandstone, adularia, hematite, clay minerals, XRD, SEM-EDS.

This report concerns a study which was conducted for SKB. The conclusions and viewpoints presented in the report are those of the authors and do not necessarily coincide with those of the client.

A pdf version of this document can be downloaded from [www.skb.se](http://www.skb.se)

# Abstract

The Swedish Nuclear Fuel and Waste Management Company (SKB) is currently carrying out site investigations in the Simpevarp/Laxemar area in the Oskarshamn region, in order to find a suitable location for long-time disposal of spent nuclear fuel. The drill core KSH03A+B from Simpevarp peninsula has been sampled for detailed studies of fracture mineralogy. The sampling of fracture fillings was focused to a major deformation zone, striking NNE-SSW, although samples were also collected from above and below this zone. Samples of a sandstone occurrence from the deformation zone were also investigated. The results from this study have been compared to the detailed fracture filling studies of drill-cores KSH01 from Simpevarp /Drake and Tullborg 2004/, KLX02 from Laxemar, KAS 04 and KA1755A from Äspö /Drake and Tullborg 2005/, KKR01, KKR02, KKR03 from Götemar /Drake and Tullborg 2006a/ and ongoing studies of drill cores KLX03, KLX04, KLX05, KLX06 and KLX07 from the Laxemar subarea /Drake and Tullborg, in manuscript/.

In order to investigate the features of the fracture fillings and their relative relations a total number of 20 thin sections and one fracture surface sample have been analysed using petrographic microscope and scanning electron microscope (SEM-EDS). Additional fracture mineral identifications have been made using X-ray diffraction. 15 calcite samples have been collected for  $\delta^{18}\text{O}/\delta^{13}\text{C}$ -analyses, and  $^{87}\text{Sr}/^{86}\text{Sr}$ -isotope analyses. The isotope studies give suggestions of formation conditions of fracture fillings from different generations and are used in the discussion of relative ages of different generations.

The deformation zone shows signs of re-activation during different events. A small part of the deformation zone is made up of mylonite, while the major part of the zone is made up of cataclasite cross-cut by later fractures filled with minerals of several generations, mainly calcite, adularia and chlorite. The cataclasite can be divided into some sub-generations of different colour and mineralogy, reflecting re-activation at different events. The major cataclasite formation is however interpreted to take place quite early. Subsequent fracture fillings also represent several generations. The earliest formed fractures that cross-cut the cataclasite are filled with calcite, adularia, laumontite, quartz, chlorite, illite, hematite, and occasionally prehnite. Stable isotope results suggest that these fillings are formed at different events during a long time sequence (from prehnite-pumpellyite facies formation conditions to even lower formation temperatures).

A later formed, better established fracture filling generation identified in KSH03 consists of calcite, adularia, chlorite, hematite, fluorite, quartz, pyrite, barite, illite/chlorite (ML-clay), corrensite, and occasionally gypsum, REE-carbonate, apophyllite, chalcopyrite, galena, sphalerite, Ti-oxide, U-silicate, laumontite, Cu-oxide and apatite. The parageneses and stable isotope results from this generation are in accordance with fracture fillings of presumed Palaeozoic age identified earlier in the area e.g. /Wallin and Peterman 1999, Bath et al. 2000, Drake and Tullborg 2004, 2005, 2006a, in manuscript, Sundblad et al. 2004, Tullborg 2004/. This fracture filling generation is found in fractures cutting the sandstone in the deformation zone. The sandstone is assumed to be Cambrian but its actual displacement to the present depth (about 230 m below the horizontal plane) has probably taken place later.

# Sammanfattning

Sprickmineralogiska undersökningar har utförts på det 1 000-m djupa kärnbrorrhålet KSH03A+B, Simpevarpshalvön, inom ramen för SKB's (Svensk Kärnbränslehantering AB) platsundersökningar. Provtagningen av sprickfyllnader fokuserades till en större deformationszon, med strykning i NNO-SSV men prover togs även ovanför och nedanför zonen. Prover från en sandstensförekomst i deformationszonen har också undersökts. Resultaten från denna studie har jämförts med detaljerade sprickmineralundersökningar från borrhål KSH01 Simpevarp /Drake and Tullborg 2004/, KLX02, Laxemar, KAS 04 och KA1755A, Äspö /Drake and Tullborg 2005/, KKR01, KKR02 och KKR03, Götömar /Drake and Tullborg 2006a/ och pågående studier av borrhål KLX03, KLX04, KLX05, KLX06 och KLX07, Laxemar /Drake and Tullborg, i manuskript/.

Totalt har 20 tunnslip från läkta sprickor och sprickytan från en öppen spricka undersökts för att utröna karaktärsdrag och relativa relationer mellan olika sprickfyllningar. Proverna har huvudsakligen undersökts med svepelektronmikroskop (SEM-EDS) och petrografiskt mikroskop. Sprickmineralidentifikationer har även utförts med röntgendiffraktion (XRD). Femton kalcitprover har valts ut för  $\delta^{18}\text{O}/\delta^{13}\text{C}$ -analys, varav ett antal prover även analyserats med avseende på  $^{87}\text{Sr}/^{86}\text{Sr}$ -innehåll. Isotopanalyserna ger information om bildningsförhållanden för sprickfyllningarna och bidrar till relativ datering av olika sprickfyllningsgenerationer.

Deformationszonen visar tecken på reaktivering vid flera olika tillfällen. Mylonit utgör en liten del av deformationszonen medan huvuddelen av zonen utgörs av "kataklasit", som klipps av senare sprickor fyllda med mineral av flera generationer, huvudsakligen kalcit, adularia och klorit. Kataklasiten kan delas upp i ett par undergenerationer med varierande färg och mineralinnehåll, vilka reflekterar reaktivering vid flera olika tillfällen. Den huvudsakliga kataklasitbildningen antas dock vara ganska gammal (prekambrisk). Senare sprickfyllningar kan även de delas in i flera generationer. De tidigast bildade sprickorna som klipper kataklasit är fyllda med kalcit, adularia, laumontit, kvarts, klorit, illit, hematit och ibland prehnit. Resultat från stabila isotoper antyder att dessa fyllningar har bildats vid flera tillfällen under en lång tidsrymd med gradvis förändrade bildningsförhållanden (från prehnit-pumpellyit facies till gradvis lägre temperaturer).

En senare mer väletablerad sprickfyllnadsgeneration som identifierats i KSH03 består bl.a. av kalcit, adularia, klorit, hematit, fluorit, kvarts, pyrit, baryt, illit/klorit (ML-clay), korrensit och ibland gips, REE-karbonat, apofyllit, kopparkis, blyglans, zinkblände, Ti-oxid, U-silikat, laumontit, Cu-oxid och apatit. Denna paragenes och stabila isotoper från denna generation stämmer väl överens med sprickfyllningar, som sannolikt är av Palaeozoisk ålder. Denna sprickgeneration har identifierats tidigare i området t.ex. /Wallin and Peterman 1999, Bath et al. 2000, Drake and Tullborg 2004, 2005, 2006a, i manuskript, Sundblad et al. 2004, Tullborg, 2004/. Dessa sprickfyllnader finns i sprickor som klipper sandstenen i deformationszonen. Sandstenen tros vara av kambrisk ålder men den aktuella placeringen av sandstenen (ca 230 m djup från horisontalplanet) har troligen skett senare än under Kambrium.

# Contents

<b>1</b>	<b>Introduction</b>	7
<b>2</b>	<b>Objective and scope</b>	9
<b>3</b>	<b>Geological background</b>	11
<b>4</b>	<b>The drill core</b>	13
<b>5</b>	<b>Equipment</b>	15
<b>6</b>	<b>Execution</b>	17
6.2	Sample preparation and analyses	17
6.2.1	Thin sections and surface samples	17
6.2.2	Calcite analyses	17
6.2.3	X-Ray Diffraction (XRD) analysis	18
<b>7</b>	<b>Results and discussion</b>	21
7.1	Fracture filling sequence	21
7.1.1	Generation 1 and 2	22
7.1.2	Generation 3	24
7.1.3	Generation 4	24
7.1.4	Generation 5	25
7.1.5	Generation 6	27
7.2	Sandstone	29
7.3	Stable isotope studies of calcite	33
7.3.1	$\delta^{13}\text{C}$ and $\delta^{18}\text{O}$	34
7.3.2	Sr-isotopes	34
<b>8</b>	<b>Summary</b>	37
<b>9</b>	<b>Acknowledgements</b>	39
<b>10</b>	<b>References</b>	41
	<b>Appendix 1</b>	45

# 1 Introduction

The Swedish Nuclear Fuel and Waste Management Company (SKB) is currently carrying out site investigations in the Simpevarp/Laxemar area in the Oskarshamn region, in order to find a place suitable for a long-time storage of spent nuclear fuel. The drill core from the 1,000-m deep bore hole KSH03A+B from the Simpevarp peninsula (Figure 1-1) has been sampled for detailed studies of fracture mineralogy. The borehole was inclined by about  $-60^\circ$  from the horizontal plane towards the south-southeast and drilled in the easternmost part of Simpevarp peninsula, in order to penetrate a lineament/deformation zone. This zone was interpreted from geophysical data to strike NNE-SSW, sub-parallel to the coast line. The sampling of fracture fillings was focused to this major deformation zone, although samples were also collected from both above and below the zone. Samples of a sandstone occurrence from the deformation zone were also investigated. As fracture fillings occur in different, often small amounts, scattered across the drill-core it is difficult to know how representative the samples are. The sampling was mainly focused on samples that give information of relative dating of fracture fillings from different generations and not to get a statistical overview of the fracture fillings. The results from this study have been compared to the detailed fracture filling studies of drill-cores KSH01 from Simpevarp /Drake and Tullborg 2004/, KLX02 from Laxemar, KAS 04 and KA1755A from Äspö /Drake and Tullborg 2005/, KKR01, KKR02 and KKR03 from Götemar /Drake and Tullborg 2006a/ and ongoing studies of drill cores KLX03, KLX04, KLX05, KLX06 and KLX07 from the Laxemar subarea /Drake and Tullborg, in manuscript/. In this report KSH03 includes both KSH03A and KSH03B.

In order to investigate the features of the fracture fillings and their relative relations a total number of 20 thin sections have been analysed using petrographic microscope and scanning electron microscope (SEM-EDS). One fracture surface sample has also been analysed using SEM-EDS. Additional fracture mineral identifications have been made using X-ray diffraction. 15 calcite samples have been collected for  $\delta^{18}\text{O}/\delta^{13}\text{C}$ -analyses, and additional  $^{87}\text{Sr}/^{86}\text{Sr}$ -isotope analyses. The isotope studies give suggestions of formation conditions of fracture fillings from different generations and support the relative dating of these generations.

The work was carried out in accordance with activity plan SKB PS 400-04-018. In Table 1-1 controlling documents for performing this activity are listed. Both activity plan and method descriptions are SKB's internal controlling documents.

**Table 1-1. Controlling documents for the performance of the activity.**

<b>Activity plan</b>	<b>Number</b>	<b>Version</b>
Sprickmineralogiska undersökningar.	AP PS 400-04-018	1.0
<b>Method descriptions</b>	<b>Number</b>	<b>Version</b>
Sprickmineralogy.	SKB MD 144.000	1.0

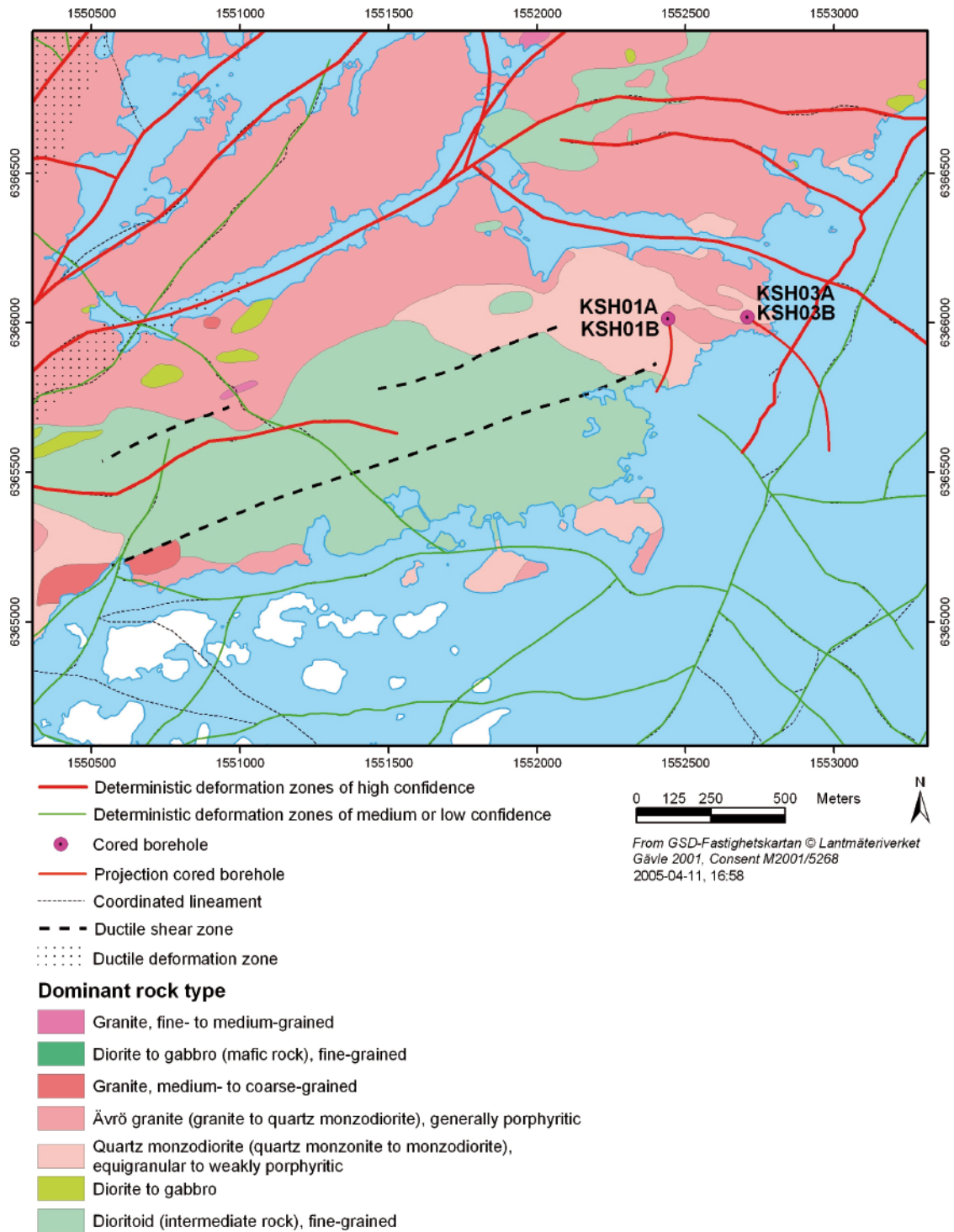


**Figure 1-1.** Geological map showing the surface-location and projection of the boreholes KSH01 and KSH03 at the Simpevarp peninsula.

## 2 Objective and scope

The aim of this study is to obtain a detailed description, including mineralogy, geochemistry, relative dating and isotopic composition, of fracture fillings from bore hole KSH03A+B. Major focus was set on investigating the pronounced deformation zone that separates the Simpevarp domain from a domain south of the zone. The major part of the deformation zone shows signs of extensive oxidation, related to semi-ductile to brittle deformation. It has a complex history and shows signs of re-activation. The major deformation in the zone is apparently associated to oxidation, with abundant hematite-rich fracture mineralization, which is a common feature on the Simpevarp peninsula /Drake and Tullborg 2004, 2006b, Wahlgren et al. 2004/. Calcite-fillings that cross-cut and postdate fracture fillings that are related to the oxidation have been sampled in order to get isotopic information, and information of the deformation history of the zone. Thin section-examinations by petrographic microscope and SEM-EDS, in combination with X-ray diffraction were the methods used for mineral identification and for discrimination of generations.

A sandstone occurrence incorporated in the zone was also sampled in order to obtain the relations between the sandstone and the deformation zone, information about how the sandstone was emplaced and its age. Samples were also taken from sections above and below the zone, respectively.

This study is done as a part of a Fil Lic project at the Department of Geology, Earth Sciences Centre, Göteborg University.



### 3 Geological background

The bedrock in the Simpevarp/Laxemar area north of Oskarshamn is dominated by Småland granitoids and dioritoids belonging to the Transscandinavian Igneous Belt (TIB) e.g. /Gaal and Gorbatshev 1987, Kornfält and Wikman 1987, Kornfält et al. 1997, Wahlgren et al. 2004/. This belt is found between the older Svecofennian (c 1.9 Ga) crust in the east-northeast and the younger, Gothian rocks in the west e.g. /Åhäll and Larson 2000/. The TIB granitoids and volcanics were emplaced and extruded during several pulses of magmatism between 1.85 and 1.66 Ga with the younger of these rocks in the west /Larson and Berglund 1992, Åhäll and Larson 2000/. TIB is divided into three major magmatic events; TIB 1 (1.81–1.77 Ga), TIB 2 (1.72–1.69 Ga) and TIB 3 (1.69–1.66 Ga) /Larson and Berglund 1992, Åhäll and Larson 2000/. The Småland granitoids in the Simpevarp/Laxemar/Äspö area belong to the TIB 1 and have been dated to 1804 $\pm$ 4 Ma (zircon) using U/Pb-isotopes /Kornfält et al. 1997/ and 1802 $\pm$ 4 Ma (zircon), 1793 $\pm$ 4 (titanite) and 1800 $\pm$ 4 Ma (titanite+zircon) /Wahlgren et al. 2004/. Another magmatic episode in the region was the intrusion of anorogenic granites, at e.g. Götemar /Kresten and Chyssler 1976, Åberg et al. 1984/ and Uthammar. These coarse-grained granites were emplaced at 1452 $\pm$ 11 $\pm$ 9 Ma (Götemar) and 1441 $\pm$ 5 $\pm$ 3 Ma (Uthammar) /Åhäll 2001/. Dating and determination of a paleomagnetic pole of the porphyritic quartz monzodiorite from Äspö HRL, show that the rock has not been heated above 550–600°C since c 1750 Ma /Maddock et al. 1993/.

The bedrock surface at the Simpevarp peninsula is dominated by the rock types “fine-grained dioritoid” in the southern part, “Ävrö granite” (with a composition from granite to quartz monzodiorite) in the eastern part and “quartz monzodiorite” (with a composition from quartz monzonite to quartzdiorite) in the northern part /Wahlgren et al. 2004/. The rock types on the Simpevarp peninsula are structurally well preserved, although some local occurrences of a decimetre to a couple of metres wide, low-grade, ductile shear zones, may occur /Wahlgren et al. 2004/. Many of the rocks have suffered from a low-grade, metamorphic alteration, visualised as sericitization and/or saussuritization of plagioclase and chloritization of biotite /Wahlgren et al. 2004/. An extensive, inhomogeneous red staining (oxidation/hydrothermal alteration) affects all rock types on the peninsula is /Drake and Tullborg 2004, 2006a, Wahlgren et al. 2004/. The dominant rock types on the Simpevarp peninsula are interpreted to be formed more or less synchronously, based on mixing and mingling relationships, diffuse contacts and ages for the quartz monzodiorite and the Ävrö granite /Kornfält et al. 1997, Wahlgren et al. 2004/.

Earlier studies of the fracture mineralogy within the Simpevarp/Laxemar site investigations have been carried out by e.g. /Drake and Tullborg 2004, 2005/. Earlier studies of fracture mineralogy in the region have been carried out by e.g. /Tullborg 1988, 1995, Alm and Sundblad 2002, Drake and Tullborg 2006a/.

## 4 The drill core

Borehole KSH03A is the third 1,000-m deep cored borehole, drilled within the site investigation program in the Simpevarp area in 2003. The borehole is telescopic implying that the upper part, 0–100 m, is percussion drilled and has a larger diameter than the core drilled part. To cover up for the missing core for the uppermost 100 m another core drilled borehole, KSH03B, was drilled adjacent to KSH03A down to 100 m. In this report KSH03 includes KSH03A plus KSH03B. The inclination of the bore hole KSH03A (KSH03B in brackets) is  $-59.09^\circ$  ( $-64.30^\circ$ ), the bearing is  $125.02^\circ$  ( $128.54^\circ$ ) and the diameter of the borehole is 76 mm.

General lithologies and a prominent deformation zone in KSH03 make up a natural subdivision of the core into three major sections /Ehrenborg and Stejskal 2004/. Section I, 0–190 m, is dominated by quartz monzodiorite. Section II, 190–300 m, is characterized by high fracture frequencies. Section III, 300–1,000 m, is dominated by Ävrö granite. The contact between the quartz monzodiorite and the Ävrö granite is located to the weakness zone in section II at 270 m. Section II is characterized by the highest frequencies of open fractures (interpreted), high numbers of joint alteration, commonly crush, almost continuous sealed fracture networks, breccia occurrences, abundance of shear structures, continuous oxidation and a section of mylonite /Ehrenborg and Stejskal 2004/. Although thinner oxidized sections occur all through KSH03 intervals with continuous oxidation, occasionally rather intense, are closely related to the quartz monzodiorite and its contact with the Ävrö granite, at 25–360 m. Three small occurrences of sandstone occur at 271.59–271.88, 271.90–271.98 m and 272.37–272.46 m within the weakness section.

In the single-hole interpretation of the bore hole three rock units are indicated, mixture of Ävrö granite and quartz monzodiorite (0–270 m), totally dominated by Ävrö granite (270–440 m, 575–755 m, 864–1,000 m) and mixture of fine- to medium-grained granite (slightly dominating) and Ävrö granite (440–575 m, 755–864 m), respectively /Hultgren et al. 2004/. According to this interpretation the major deformation zone is characterised by inhomogeneous, low-grade, ductile deformation, high frequency of open and sealed fractures and crush zones with brecciation between 220–235 m and mylonitization between 270–275 m.

## 5 Equipment

### 5.1 Description of equipment

The following equipment was used in the fracture mineralogy investigations of samples from drill core KSH03.

- Scanning electron microscope (Zeiss DSM 940) with EDS (Oxford Instruments Link).
- Microscopes (Leica DMRXP and Leica DMLP).
- Stereo microscope (Leica MZ12).
- Microscope camera (JVC TK-1280E).
- Digital camera (Konica Revio KD-420Z).
- Stone cutter.
- Magnifying lens – 10x.
- Scanner (Epson 3200) and Polaroid filters.
- Computer software, e.g. Corel Draw 11, Microsoft Word, Microsoft Excel, WellCad, BIPS, Link ISIS.
- Stable carbon and oxygen isotope analysis equipment.

All of the equipment mentioned above is property of the Earth Sciences Centre, Göteborg University, SKB or the authors.

External laboratory equipment was used for:

- Analyses of  $^{87}\text{Sr}/^{86}\text{Sr}$ -isotopes from calcite.
- X-Ray Diffraction-analyses.

See chapter “execution” for more details.

## 6 Execution

### 6.1 Sample collection

Samples suitable for fracture mineral investigations were collected from the drill core. The samples were collected throughout the drill core, with a focus on the deformation zone. The length of the samples ranges from 4 to 35 cm.

### 6.2 Sample preparation and analyses

#### 6.2.1 Thin sections and surface samples

The samples were photographed and sawed. All together 20 thin sections (Table 6-1) were prepared by Ali Firoozan, Earth Sciences Centre, Göteborg University and by Kjell Helge, Minoprep AB, respectively. The thicknesses of the thin sections were about 30  $\mu\text{m}$  except for sample 186.52–186.62 m, which has a thickness of about 100  $\mu\text{m}$ . The thin sections were scanned with Epson 3200 scanner, using Polaroid filters, in order to optimize SEM-EDS investigations. The prepared samples were initially examined with petrographic microscope. Selected parts of the samples were photographed with microscope camera.

The thin sections (and one sample of a fracture surface) were examined in detail and analysed using an Oxford Instruments energy dispersive system mounted on a Zeiss DSM 940 SEM at the Earth Sciences Centre, Göteborg University, Sweden. Polished thin-sections were coated with carbon for electron conductivity. The acceleration voltage was 25 kV, the working distance 24 mm and the specimen current was about 0.7 nA. The instrument was calibrated at least twice every hour using a cobalt standard linked to simple oxide and mineral standards, to confirm that the drift was acceptable. ZAF calculations were maintained by an on-line LINK ISIS computer system. These quantitative analyses give reliable mineral compositions but  $\text{Fe}^{2+}$  and  $\text{Fe}^{3+}$  are not distinguished and the  $\text{H}_2\text{O}$  content is not calculated. Detection limits for major elements are higher than 0.1 oxide %, except for  $\text{Na}_2\text{O}$  with a detection limit of 0.3%.

#### 6.2.2 Calcite analyses

The stable carbon and oxygen isotope analyses carried out at the Earth Sciences Centre, Göteborg University, on 15 calcite samples (Table 6-1) were made accordingly: Samples, usually between 150 and 250  $\mu\text{g}$  each, were roasted in vacuum for 30 minutes at 400°C to remove possible organic material and moisture. Thereafter, the samples were analysed using a VG Prism Series II mass spectrometer with a VG Isocarb preparation system on line. In the preparation system each sample was reacted with 100% phosphoric acid at 90°C for 10 minutes, whereupon the released  $\text{CO}_2$  gas was analysed in the mass spectrometer. All isotope results are reported as  $\delta$  per mil relative to the Vienna Pee Dee Belemnite (VPDB) standard. The analyse-system is calibrated to the PDB scale via NBS-19.

Göran Åberg at Institute for Energy Technology, Norway, carried out the Sr-isotope analyses and preparation according to the following procedure. About 30 to 40 mg of the 6 carbonate samples (Table 6-1) were transferred to 2 ml centrifuge tubes, added 200  $\mu\text{l}$  0.2 M HCl, and shaken. The samples were let to react for 10 minutes while shaken in order to release the  $\text{CO}_2$  gas. If not completely dissolved 20  $\mu\text{l}$  2 M HCl is added once or twice

until most of the calcite has been decomposed. The samples were centrifuged for about 4 minutes and the liquids transferred to new clean centrifuge tubes by use of a pipette. New pipette tips are used for each sample. The centrifuge tubes are put on a hotplate and evaporated to dryness. To avoid disturbances in measuring the isotopic composition, strontium had to be separated from other elements present in the sample. After evaporation to dryness the samples were dissolved in 200  $\mu$ l ultrapure 3M HNO<sub>3</sub>, centrifuged and loaded onto ion-exchange columns packed with a Sr-Spec crown-ether resin from EICrom, which retained Sr and allowed most other elements to pass. After rinsing out the remaining unwanted elements from the columns, strontium was collected with ultrapure water (Millipore). The collected Sr- fractions were then evaporated to dryness and loaded on pre-gassed Re filaments on a turret holding 12 samples and 1 NIST/NBS 987 Sr standard. The isotopic composition of Sr was determined by thermal ionization mass spectrometry (TIMS) on a Finnigan MAT 261 with a precision of about 20 ppm and a Sr blank of 50–100 pg. The <sup>87</sup>Sr/<sup>86</sup>Sr ratio of the carbonate analysis are monitored by analysing one NIST/NBS SRM 987 Sr standard, for each turret of 12 samples, and the standard has a recommended <sup>87</sup>Sr/<sup>86</sup>Sr value of 0.710248. The presented results are not corrected to the NBS 987 recommended value but given together with the specific measured NBS 987 value for the relevant turret.

### 6.2.3 X-Ray Diffraction (XRD) analysis

For the 8 XRD analyses (Table 6-1) the fracture material was scraped off the fracture walls or from sealed fracture fillings. The amounts of the different samples were highly variable.

Sven Snäll at SGU, Uppsala, Sweden, carried out the analyses according to the following procedure. The clay-rich samples were dispersed in distilled water, filtered and oriented according to /Drever 1973/. In samples of small volumes the suspension was repeatedly put on glass and dried. Three measurements were carried out on each of the fine fraction samples for clay mineral identification; 1) dried samples 2) saturated with ethyleneglycol for two hours and finally 3) after heating to 400°C in two hours. Coarser material was wet sieved and dried. The > 35 $\mu$ m fraction was ground by hand in an agate mortar. The sample powder was randomly orientated in the sample holder (or on a piece of glass if very small sample volumes). The radiation (CuK $\alpha$ ) in the diffractometer was generated at 40 kV and 40 mA, and the X-rays were focussed with a graphite monochromator. Scans were run from 2°–65° (2-theta) or from 2°–35° (samples with preferred crystal orientation) with step size 0.02° (2-theta) and counting time 1 s step<sup>-1</sup>. The analyses were performed with a fixed 1° divergence and a 2 mm receiving slit. The XRD raw files were taken up in the Bruker/Siemens DIFFRAC<sup>PLUS</sup> software (version 2.2), and evaluated in the programme EVA. The minerals were identified by means of the /PDF 1994/ computer database.

**Table 6-1. Investigation techniques used for each sample. <sup>1</sup> = including a fracture surface sample, <sup>2</sup> = calcite.**

Sample	Thin Section	XRD	$\delta^{18}\text{O}$ and $\delta^{13}\text{C}^2$	$^{87}\text{Sr}/^{86}\text{Sr}^2$
14.97–15.32	X	X	X	
111.80–111.92	X		X	X
117.75–117.94		X	X	
126.00–126.22	XX		X	
159.69		X		
177.74–177.81	XX		XX	X
180.03		X		
181.93–181.98	X	X	XX	X
186.52–186.62	X		X	
197.79–197.85	X		X	
220.15–220.31	X	X	X	X
225.44–225.49	X		X	X
233.56–233.67	X			
245.03–245.07	X			
269.77–269.94	X			
271.53–271.63	XX			
295.80–296.07	X			
305.64–305.76	X		XX	
340.92–341.06	X			
495.42		X		
684.46		X		
863.66–863.84	X <sup>1</sup>		X	X
Number of samples	20	8	15	6

## 7 Results and discussion

In this section, results from thin section analyses, X-ray diffraction and stable isotopes are presented and discussed. Relative ages of different fracture filling generations are shown in a schematic sequence of fracture filling events (Table 7-1). The results from KSH03 in comparison to earlier and ongoing works in the area e.g. /Tullborg 1988, 1997, Drake and Tullborg 2004, 2005, 2006a, in manuscript/ show that the general fracture mineralogical features and occurrences are similar throughout the Simpevarp-Laxemar-Äspö area, although differences exist. The major difference is that the Simpevarp subarea is characterized by a higher degree of brittle deformation, resulting in breccias and cataclasites and generally higher fracture frequencies compared to the Laxemar subarea. The major deformation zone in drill core KSH03 is characterized by deformation and fracture filling features which are somewhat different from the general features of the Simpevarp, Laxemar and Äspö areas.

Thin section descriptions with images, X-ray diffraction results and stable isotope results are found in the Appendix.

### 7.1 Fracture filling sequence

The characteristics of the fracture fillings identified in KSH03 (Table 7-1) is presented in this section. Similarities and differences compared to earlier studies and relative differences within the different drill core sections in KSH03 will to some extent also be discussed. Sampling was focused on the major deformation zone in the drill core, a zone that is characterized by mostly brittle (to semi-ductile) deformation resulting in extensive brecciation and cataclasite formation. The zone has been re-activated several times, resulting in cataclasites, breccias and fracture fillings of several generations.

The fracture filling sequence presented below (Table 7-1) has been reworked from /Drake and Tullborg 2005/ and includes results from this study. The sequence comprises a relative chronological sequence of the characteristic minerals in each fracture filling generation from the Simpevarp, Laxemar and Äspö areas, with results from drill core KSH03 along with results from drill cores KSH01 /Drake and Tullborg 2004/, KLX02, KAS04, KA1755A /Drake and Tullborg 2005/, KKR01, KKR02, KKR03 /Drake and Tullborg, 2006a/, KLX03, KLX04, KLX05, KLX06 and KLX07 /Drake and Tullborg, in manuscript/. Only a few of the minerals in each generation is commonly observed in a single sample. The relative abundance of the minerals in each generation varies widely between different samples. The most common fracture minerals, present in most of the generations, are calcite and chlorite. These minerals have precipitated at several events under different conditions. Stable isotope analyses of calcite provide information of these conditions and from which type of fluid the calcite precipitated, which gives input to the discussion about the relative age of the fracture filling generations. SEM-EDS analyses of chlorite reveal differences in chemistry between chlorite from different generations. K-feldspar, clay minerals and hematite are common in the major deformation zone compared to the surrounding rock. These minerals are commonly found in sealed fracture networks (sometimes cataclastic) and as gouge material in open or sealed fractures and are characterized by a dark red to brown colour.

**Table 7-1. Schematic fracture filling-sequence from Simpevarp/Laxemar/Äspö/ (Götemar). Minerals identified in KSH03 samples in *italic* letters. The most abundant minerals in each generation are in bold letters. Minerals in brackets are only found occasionally.**

- 
1. **Quartz- and epidote-rich mylonite**, occasionally including muscovite, titanite, Fe-Mg-chlorite, *albite*, (apatite), (calcite), (*K-feldspar*).
  2. **Cataclasite**
    - a. Early **epidote-rich**, with quartz, titanite, Fe-Mg-chlorite, (*K-feldspar*), (*albite*).
    - b. Late **hematite-rich**, with epidote, **K-feldspar**, quartz, *albite*, **chlorite**.
  3. Euhedral **quartz**, **epidote**, **Fe-Mg chlorite**, **calcite**<sup>1</sup>, pyrite, fluorite, muscovite, (*K-feldspar*).
  4. **Prehnite**, (fluorite).
  5.
    - a. **Calcite**<sup>2</sup>, (fluorite, hematite).
    - b. **Dark red/brown filling - Adularia, Mg-chlorite** (also as ML-clay with Illite), **hematite** (quartz), (*apatite*); sometimes cataclastic.
    - c. **Calcite**<sup>3</sup>, **adularia, laumontite, Mg-chlorite, quartz, illite** (also as ML-clay with chlorite), **hematite**, (*albite*).
  6. **Calcite**<sup>4</sup>, **adularia, Fe-chlorite, hematite, fluorite, quartz, pyrite, barite, gypsum**, harmotome, REE-carbonate, apophyllite, illite/chlorite (ML-clay), corrensite, chalcopyrite, galena, sphalerite, Ti-oxide, U-silicate, laumontite, Cu-oxide, sylvite, (Fe-oxyhydroxide), (Mg-chlorite), (*apatite*), (wolframite).
  7. **Calcite**<sup>5</sup>, pyrite.
- 

<sup>1</sup> = Commonly coarse-grained euhedral with abundant twinning lamellae and signs of deformation/alteration.

<sup>2</sup> = Euhedral to subhedral crystals with abundant twinning lamellae, filling prehnite coated fractures.

<sup>3</sup> = Commonly as subhedral crystals with abundant twinning lamellae, filling space in narrow fractures.

<sup>4</sup> = Commonly as fine-grained subhedral crystals with a small number of twinning lamellae, filling space in undulating and very narrow fractures. Scalenohedral crystal shapes on fracture surfaces (Possibly Palaeozoic).

<sup>5</sup> = Crystals in open fractures and voids.

The characteristics of each fracture filling generation are described below. Fracture filling generation 7 was not sampled in this study.

### 7.1.1 Generation 1 and 2

A mylonite (generation 1, Table 7-1) sampled from below the deformation zone in the drill core at 863.66–863.84 m, was investigated in this study. This mylonite is rich in epidote and subordinately quartz, in a fine-grained groundmass. Fragments consist of more coarse-grained K-feldspar and quartz. It is similar to the mylonites from Äspö Shear Zone /Drake and Tullborg 2005/ although it is less extensive than the mylonites at Äspö. Similar homogenous mylonites are not very common in the Simpevarp subarea.

SEM-EDS analyses (see Appendix) of epidote crystals show that they are relatively Fe-poor, in accordance to earlier studies of epidote in mylonites /Drake and Tullborg 2004, 2005/. This is in contrast to the more Fe-rich epidote, which have precipitated subsequently to the mylonite formation. A small part of the deformation zone is mapped as mylonite. This part was not sampled. This mylonite is darker and probably more chlorite rich than e.g. mylonite in the Äspö Shear Zone /Drake and Tullborg 2005/.

Cataclasites (generation 2, Table 7-1) are found in at least two varieties. One is green, epidote-rich and contains epidote, albite, K-feldspar and quartz and the other is more brownish and hematite-rich (Figure 7-2). The hematite-rich cataclasite consists mainly of adularia, chlorite, hematite, quartz, albite and epidote. The cataclasites make up narrow, often re-activated, fracture networks and often feature a grain-size reduction in the adjacent wall rock.





**Figure 7-1.** Photo of drill core sample 863.66–863.84 m. Several parallel fractures, filled with quartz and K-feldspar and chlorite (dark), are cutting through a fine-grained, epidote-rich mylonite with fragments of quartz and K-feldspar. Width of photo is 35 mm. The arrow shows the position of the SEM-image in Figure 7-3 below.



**Figure 7-2.** Drill core sample showing hematite-rich cataclasite (brownish red) and epidote-rich cataclasite (green), that are cut by fractures filled with calcite and adularia. Sample 305.64–305.76 m. Drill core diameter is about 50 mm.

Included in the cataclasites are often angular fragments of the wall rock. The cataclasites are formed at brittle conditions, although some semi-ductile features are also identified. Similar cataclasites have been described from drill core KSH01 /Drake and Tullborg 2004/. The epidote-rich cataclasite is probably somewhat older than the hematite-rich cataclasite, based on cross-cutting relations.

It seems likely that the hematite-rich cataclasite is formed at more than one event e.g. based on the fact that prehnite predated the hematite-cataclasite formation (observations from KSH01) whereas investigations from KSH03 show that prehnite also post-date hematite-cataclasite. A later formed hematite-rich filling also consisting of adularia, Mg-rich chlorite and calcite (generation 5, Table 7-1) is very similar in appearance and mineralogy to the hematite-cataclasite. This later formed filling is however commonly not cataclastic, see below.

The cataclasites are commonly cut by at least three generations of calcite fillings, with different paragenetic minerals. Since the deformation zone is highly re-activated it is difficult to discern different cataclasites and breccia-sealings as well as low-temperature fillings from each other.

### 7.1.2 Generation 3

This fracture filling generation (Table 7-1) is only found in sample 863.66–863.84 m, where a fracture filled with quartz, K-feldspar and Fe-Mg-chlorite cuts through epidote-rich mylonite. K-feldspar and quartz coat the fracture walls of the chlorite-filled fracture and are thus considered to be formed earlier than chlorite. K-feldspar has not been found as a major mineral in this generation in earlier studies from Simpevarp, Laxemar or Äspö /Drake and Tullborg 2004, 2005/. The K-feldspar is red-stained due to numerous fine-grained inclusions, generally below the resolution of the SEM.

The Fe-Mg-chlorite is chemically similar to Fe-Mg-rich chlorite of generation 3 from Simpevarp, Laxemar and Äspö (Figure 7-3) /Drake and Tullborg 2004, 2005/ (Figures 7-4, 7-5).

### 7.1.3 Generation 4

Prehnite is only found in two of the studied samples in connection to the zone, 126.00–126.22-2 and 177.74–177.81-2. Studies of the wall rock alteration in e.g. KSH03 /Drake and Tullborg 2006b/ show that prehnite is abundant in fractures above the deformation zone and possibly less abundant below the zone, although still existing. SEM-EDS analyses of the sampled prehnite are in accordance with prehnite analyses from earlier works in the area /Drake and Tullborg 2004, 2005/. No fluorite was identified in relation to prehnite in these samples.

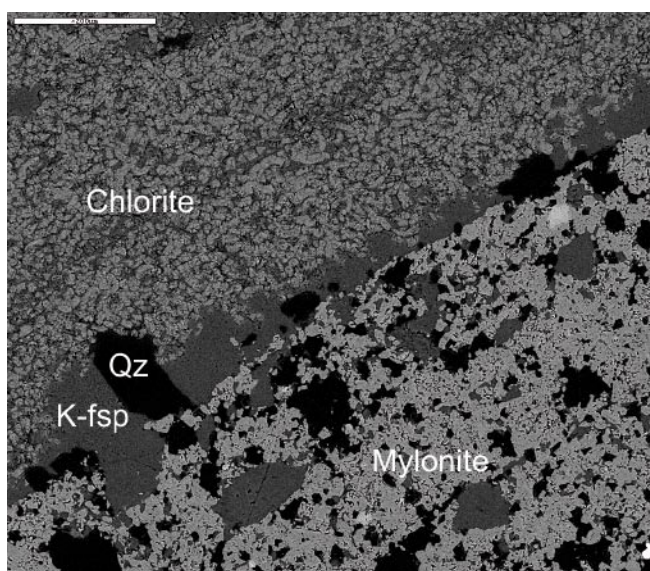


**Figure 7-3.** Back-scattered SEM-image of the epidote-rich mylonite in Figure 7-1. The mylonite is cut by a fracture coated by K-feldspar (K-fsp) and quartz (Qz). The fracture is sealed by Fe-Mg-chlorite. Scale marker bar is 200  $\mu$ m.

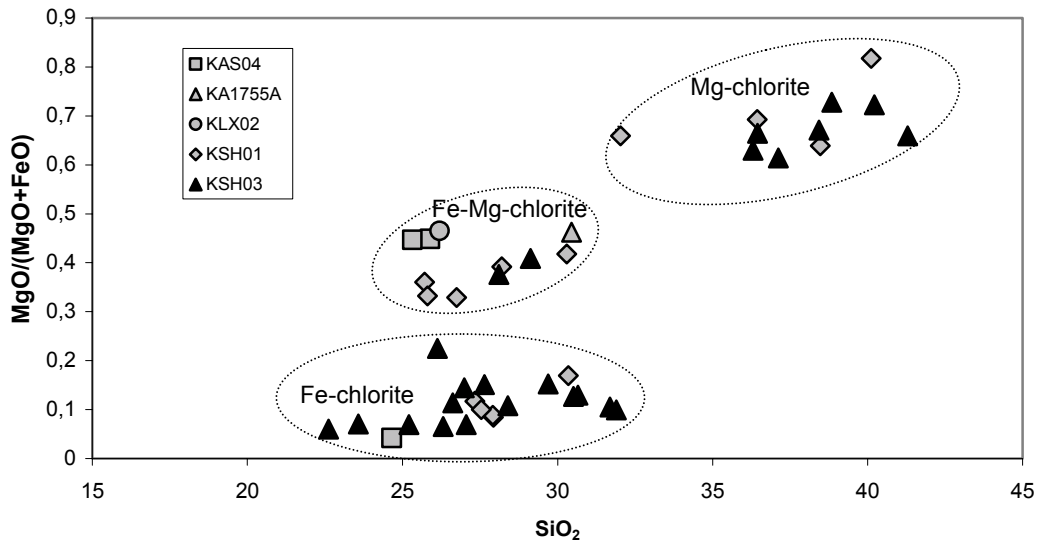


**Figure 7-4.** Plot of  $MgO/(MgO+FeO)$  vs  $SiO_2$  from SEM-EDS-analyses of chlorites from KSH03 and chlorites from drill cores KSH01, KLX02, KAS04 and KA1755A /Drake and Tullborg 2004, 2005/.

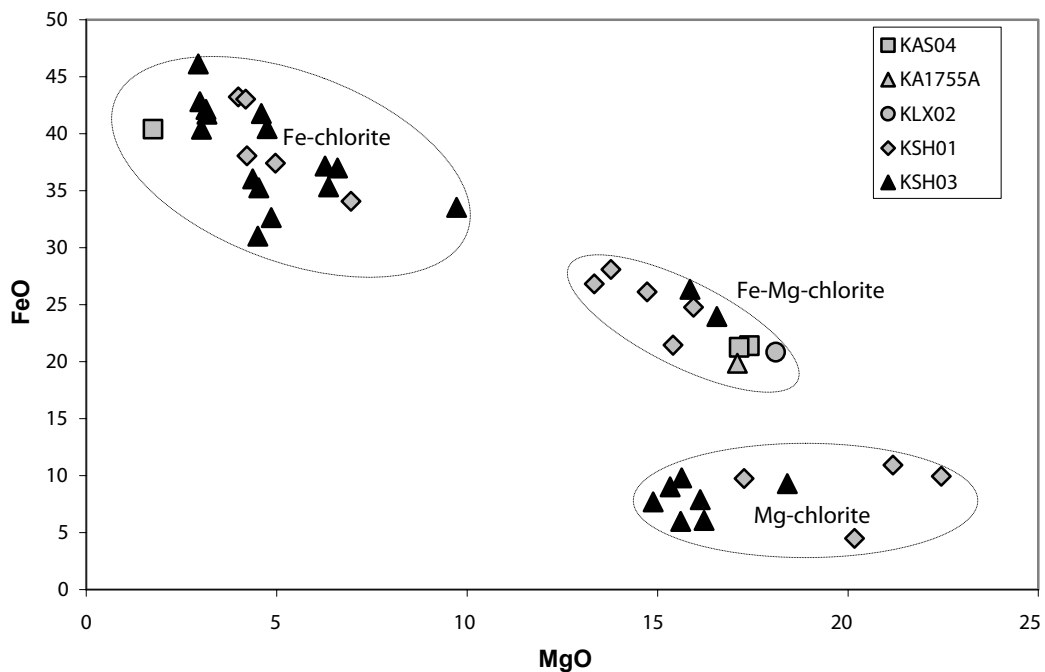


**Figure 7-5.** Plot of  $FeO$  vs  $MgO$  from SEM-EDS-analyses of chlorites from KSH03 and chlorites from drill cores KSH01, KLX02, KAS04 and KA1755A /Drake and Tullborg 2004, 2005/.

#### 7.1.4 Generation 5

Fracture filling generation 5 (Table 7-1) is the most difficult to distinguish in the present study. Stable isotope analyses of calcite (Chapter 7-3) indicate that the fillings are formed at several events. Re-activation of the deformation zone, with calcite and hematite-rich fillings of several generations makes it difficult to relate different fillings to specific generations. Most of the fillings rich in calcite, adularia, laumontite, illite, and hematite (Figures 7-6, 7-7, 7-8 and “calcite1” in Figure 7-9) postdate dark red/brown fillings (sometimes cataclastic), which are rich in adularia, Mg-chlorite (also as ML-clay with illite) and hematite.

SEM-EDS investigations and X-ray diffraction analyses show that these dark red/brown fillings in the deformation zone consist of quartz, albite, K-feldspar, epidote, Mg-rich chlorite, hematite and illite (see Appendix). Quartz, albite and some of the epidote and K-feldspar are most probably fragments from the wall rock or earlier fracture fillings.

The calcite normally shows moderately to high amount of twinning-lamellae (Figures 7-6, 7-7). Laumontite and adularia often coat the fractures that are later filled by calcite.

However, these three minerals are generally thought to be coeval. The paragenesis of calcite, adularia, Mg-rich chlorite, laumontite and illite has been documented earlier from Simpevarp, Laxemar and Äspö /Drake and Tullborg 2004, 2005/ but is thought to be most prominent in the Simpevarp area. The Mg-rich chlorite in this paragenesis is similar in composition to the chlorite found in earlier formed hematite-rich fillings and hematite-cataclasite. The analysed Mg-rich chlorite is similar to Mg-rich chlorite from KSH01, KLX02, KAS04 and KA1755A (Figures 7-4 and 7-5).

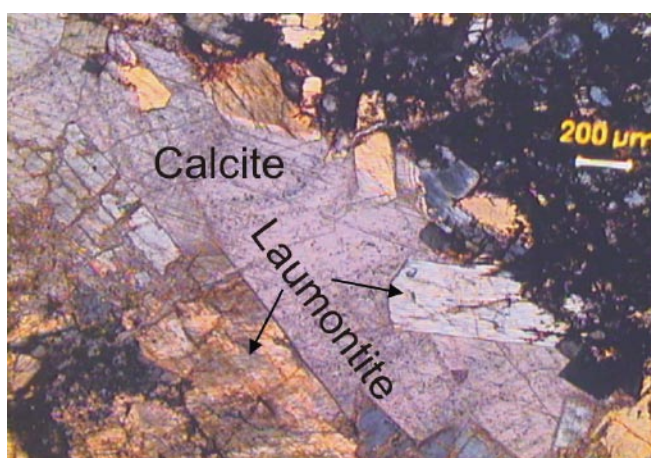


**Figure 7-6.** Microphotograph of a laumontite and calcite filled fracture that cuts through earlier formed hematite-cataclasite. Sample 177.74–177.81-1 m.

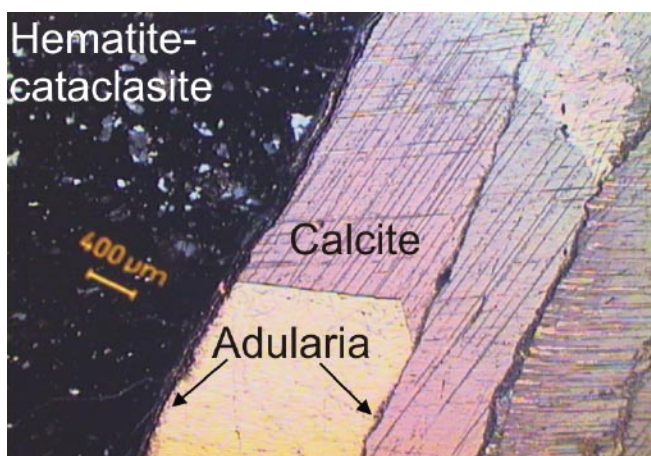


**Figure 7-7.** Microphotograph (sample 220.15–220.31 m) of a fracture filled with adularia and calcite that cuts through earlier formed hematite-cataclasite.

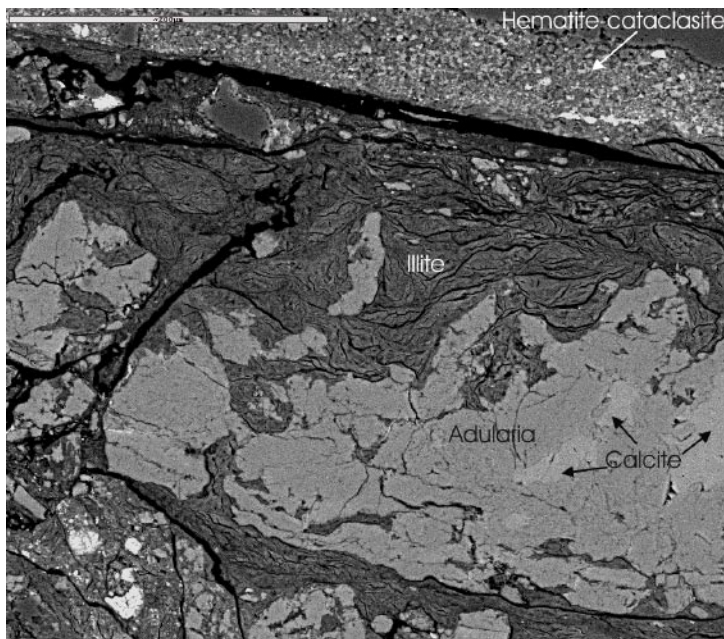


**Figure 7-8.** Back-scattered SEM-image of a fracture filled with illite, adularia and calcite that cut through earlier formed hematite-cataclasite. Sample 245.03–245.07 m. Scale marker bar is 200  $\mu\text{m}$ .

### 7.1.5 Generation 6

Thin fractures that cut through calcite, laumontite, adularia etc of generation 5 are commonly filled with calcite of generation 6 (Table 7-1 and “calcite2” in Figure 7-9). The calcite is often found together with fluorite, adularia, Fe-chlorite, hematite, fluorite, barite (Figure 7-10). REE-carbonate, illite/chlorite (ML-clay), corrensite, pyrite, chalcopryrite, U-silicate, galena, sphalerite, laumontite, Cu-oxide and apatite are occasionally found in paragenesis with calcite as well. The calcite has a low amount of twin-lamellae and is commonly found as c-axis elongated crystals with scalenohedral morphology in open fractures. This paragenesis has been found in the area (Simpevarp, Laxemar, Äspö and Götemar) in different compositions /Drake and Tullborg 2004, 2005, 2006a, in manuscript/. The calcite-fluorite filling may be related to fracture fillings described from the Götemar granite, where fractures cut through Palaeozoic sandstone /Alm and Sundblad 2002, Drake and Tullborg 2006a/. Calcite-fluorite fillings in the Götemar granite, dated to  $405 \pm 27$  Ma /Sundblad et al. 2004/ are thought to be coeval with fillings of generation 6 in KSH03, based on stable isotope results and mineral paragenesis /Drake and Tullborg 2006a and this study/. Fluid inclusions in these fillings from Laxemar and Götemar also show similar results /Alm and Sundblad 2002, Milodowski et al. 2005/. The chemistry of Fe-rich chlorite of generation 6 resembles Fe-rich chlorite found in other parts of the area (Figures 7-4 and 7-5) and in the Götemar granite /Drake and Tullborg 2006a/.

Apophyllite and gypsum, found below the major deformation zone in the drill core is also thought to be related to generation 6, based on studies by /Drake and Tullborg 2004, 2005, in manuscript/. These minerals have also been described from Laxemar /Drake and Tullborg 2005, in manuscript/ but hardly from Simpevarp which might indicate that gypsum and apophyllite crystals have been dissolved and flushed away to a high degree in the Simpevarp subarea but remains in some fractures in the Laxemar subarea.

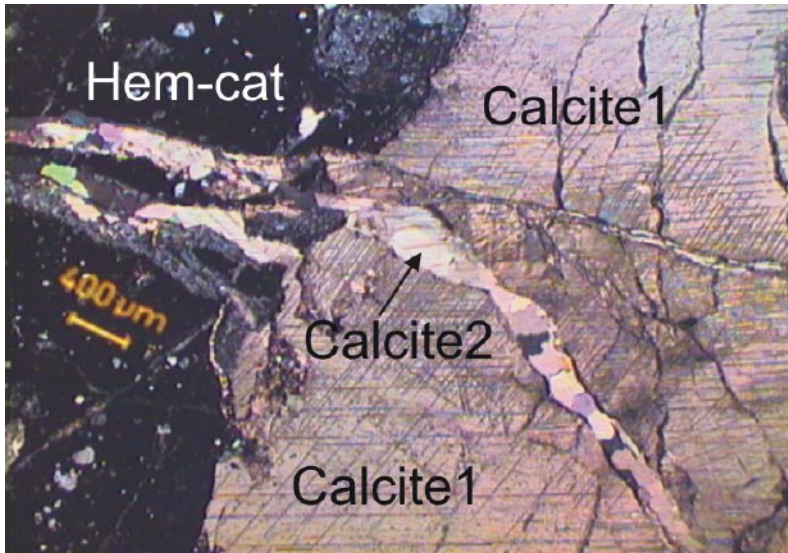


**Figure 7-9.** Microphotograph of calcite (“Calcite1”) that fills a fracture that is cutting through hematite-cataclasite (“Hem-cat”). Thin fractures that cut through “Calcite1” and hematite-cataclasite are filled with calcite (“Calcite2”) and adularia. Note the small amount of twin-lamellae in “Calcite2” compared to “Calcite1”. Sample 220.15–220.31 m.

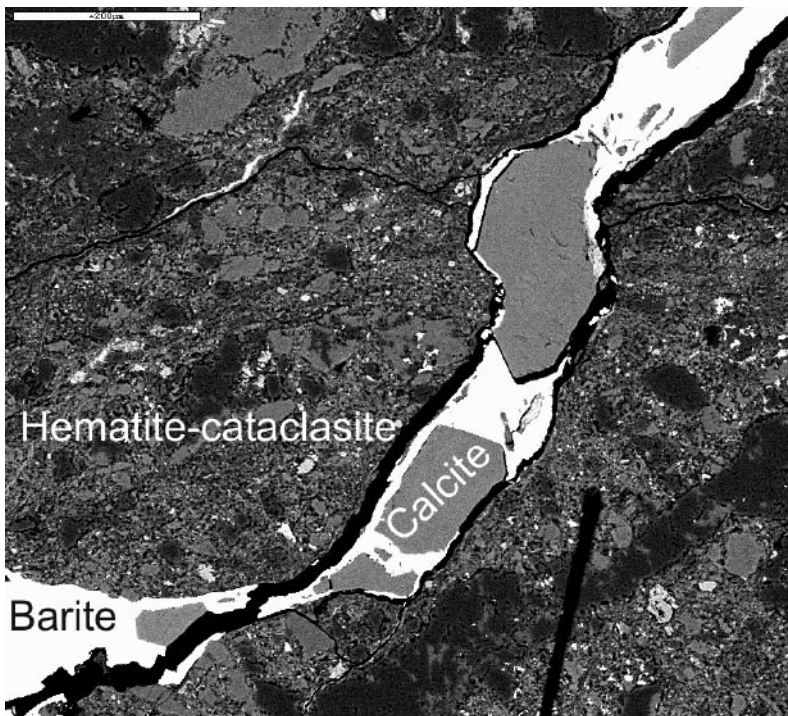


**Figure 7-10.** Back-scattered SEM-image of a fracture filled with calcite and barite that cut through earlier formed hematite-cataclasite. Sample 220.15–220.31 m. Scale marker bar is 200 µm.

## 7.2 Sandstone

Three sandstone occurrences, together comprising about 40–50 cm is found in the drill core at 271–273 m, which is close to the quartz monzodiorite/Ävrö granite contact. The vertical depths of the sandstone occurrences are about 230–235 m, since the bore hole is inclined c 60° from the surface. It is impossible to trace whether the sandstone is part of a continuous sheet-like dyke or not since it is only observed in the drill core. Sandstone has not been detected in any of the other drill cores in the Laxemar/Äspö/Simpevarp area, although an observation of a sandstone filled fracture deformed in a brittle manner, has been documented on an outcrop on the Simpevarp peninsula. The sandstone in KSH03 is bordered by red-coloured cataclasite/gouge (Figure 7-11). A green-coloured zone is occasionally found between the cataclasite and the sandstone. Two thin sections of the sandstone have been investigated by the authors and Mikael Erlström, SGU.

The sandstone is partly very loose and consists of clasts of rounded, dominantly monocrystalline quartz crystals and a fine-grained cement of dominantly quartz. Open pores are abundant. The sorting is moderate with a bimodal grain-size of a) 0.5–0.8 mm and b) 0.1–0.3 mm. The clasts of the coarser fraction are often well-rounded. K-feldspar crystals are occasionally found as clasts or as fine-grained crystals in the pore space between the quartz clasts. The sandstone is more or less entirely made up of quartz in its unaltered parts. The matrix contains fine-grained clastic clay material and the matrix content is below 5%. Clay clasts are possibly present. Accessory phases are e.g. zircon and opaque minerals. No major dissolution or re-crystallisation of the quartz clasts is observed which indicates that the sandstone has not been affected by high pressure and temperature.

### *Cataclasite and green-coloured fillings*

A very fine-grained cataclasite of hematite-stained K-feldspar and subordinate chlorite, albite, illite, hematite, is bordering the sandstone. The age of primary cataclasite formation is presumed to be Pre-Cambrian, possibly Meso-Proterozoic, although uncertain.



**Figure 7-11.** Photo of the drill core showing sandstone (grey, left side and right side) in relation to hematite-rich cataclasite (red, in the middle). The sandstone section on the right hand side is very loose and that some sandstone is incorporated in the cataclasite. Drill core diameter is about 50 mm.

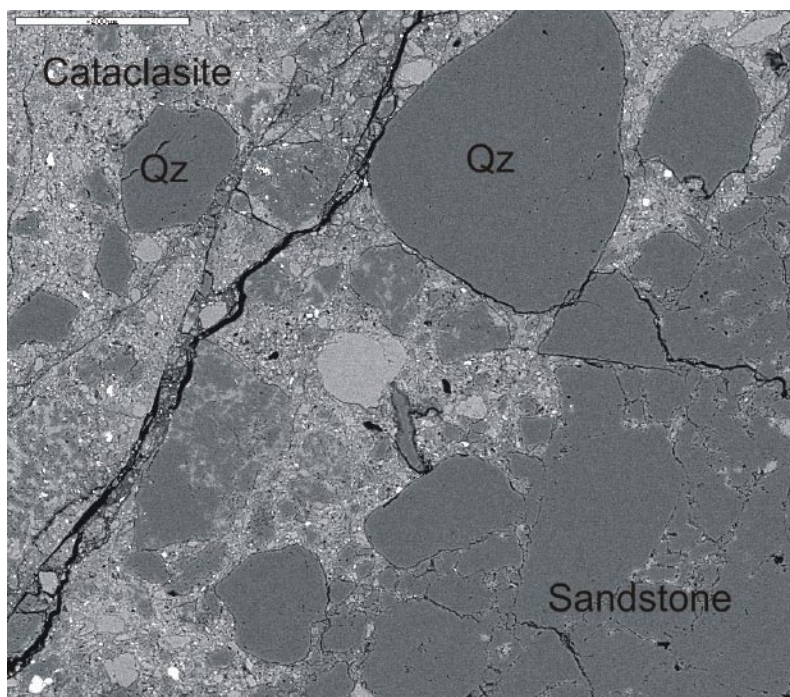


**Figure 7-12.** Back-scattered SEM-image of contact zone between cataclasite and sandstone. Rounded sandstone clasts (Qz) are incorporated in the cataclasite. Scale marker bar is 200  $\mu\text{m}$ . Sample 271.53–271.63 m (I).

A green coloured filling between the cataclasite and the sandstone consists of mainly K-feldspar (both as large subhedral crystals and as fine-grained crystals), illite (possibly in mixed layer-clay with chlorite) and subordinate Ti-oxide, albite, hematite, chlorite and fragments of quartz and apatite. However, some of the green fillings may be primary argillaceous matrix of the sandstone but most of the green filling seems to be related to the cataclasite. The angular fragments of mainly K-feldspar suggest that the filling does not originate from the same source as the sandstone. The green-coloured filling generally contains more angular quartz clasts, and a higher matrix content with a higher amount of clay minerals, mainly illite, than the sandstone in general.

#### *The border zone between sandstone and cataclasite*

The cataclasite partly penetrates the sandstone. Rounded and subordinately angular quartz crystals from the sandstone are present within the cataclasite and in higher amounts closer to the sandstone contact (Figure 7-12). An enhanced alteration is observed in the sandstone close to the cataclasite. This corresponds to an increased distance between the generally more angular quartz clasts and more K-feldspar in the cement between the clasts. The cement in the altered part of the sandstone resembles the cataclasite in mineral composition although the cataclasite is richer in hematite. Sometimes this cement constitutes a green-coloured filling that seems to penetrate through the sandstone.

The green filling between the unaltered sandstone and the cataclasite (Figure 7-13) may have been exposed to shear or mechanical stress along the contact, which resulted in a mixing between the sediment and the cataclasite, an increased matrix content, formation/re-crystallisation of clay minerals and mechanical break-down of the quartz clasts to a more angular shape. This green filling sometimes appears to be the matrix of the sandstone in the more altered parts of the sandstone. Sometimes it seems as the green-coloured filling incorporates sandstone fragments. These different features make interpretations complicated.



### *Calcite and fluorite filled fractures*

Calcite, fluorite and small amounts of REE-carbonate fill thin fractures that penetrate the sandstone, and the cataclasite (Figure 7-14). This fracture filling belongs to generation 6 (Table 7-1), and similar calcite-fluorite filled fractures that cut through Cambrian sandstone fractures have been documented from the Göttemar granite, and are generally considered to have a Cambrian maximum age e.g. /Alm and Sundblad 2002, Röshoff and Cosgrove 2002, Drake and Tullborg 2006a/. Fluorite from Göttemar fractures has been dated to  $405 \pm 27$  Ma /Sundblad et al. 2004/, which also should be the minimum age of the sandstone.

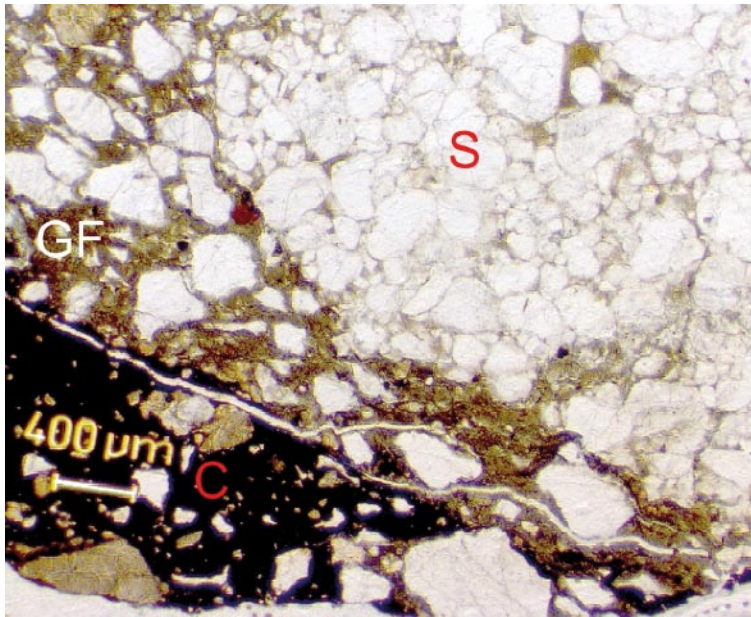


**Figure 7-13.** Microphotograph of a green-coloured filling (GF) in the border zone between cataclasite (C) and sandstone (S). The green-coloured filling has a high matrix-content. The matrix mostly consists of K-feldspar and illite and fragments are made up of more angular quartz clasts than in the sandstone. Plain polarized light. Sample 271.53–271.63 m (I).

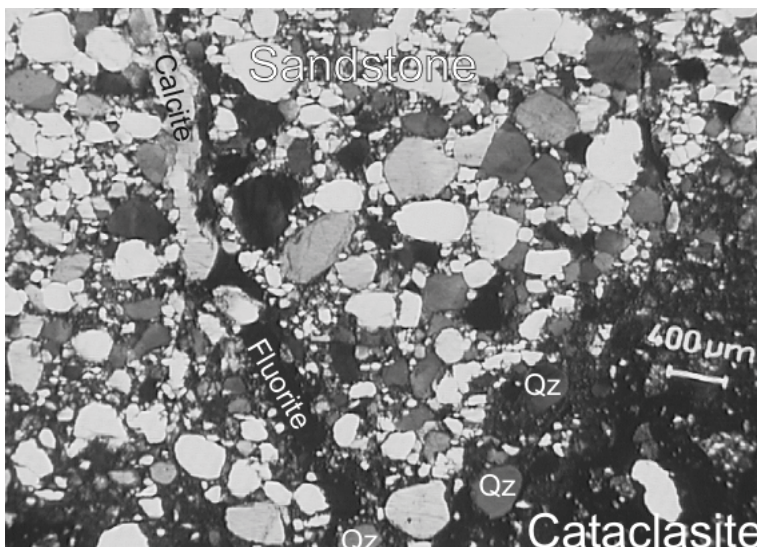


**Figure 7-14.** Microphotograph of calcite and fluorite that fills a fracture that is cutting through cataclasite and sandstone. Fragments of the sandstone (Qz) are incorporated in the cataclasite. Sample 271.53–271.63 m (I).(+nic)

### *Interpretations and timing*

The age of the sandstone is somewhat uncertain. The closest outcrop of sandstone is the Cambrian sandstone found some tens of kilometres from the shoreline in the Baltic Sea e.g. /Flodén 1980/. An early Palaeozoic cover of at least some hundreds of metres is suggested to have covered the area /Lindström 1991/. Cambrian sandstone has also been found in narrow fractures in outcrops throughout the Oskarshamn region cf /Röshoff and Cosgrove 2002/. The lower Cambrian sandstone is very pure, good sorted, with high quartz-content and low feldspar-content. The colour is white or somewhat greyish, occasionally with greenish clay laminas, as described from a drill core from Böda Hamn, Öland (about 30 km from the site investigation area) /Hessland 1955/. This description corresponds very well to the sandstone occurrence in drill core KSH03.

The fact that the sandstone is found at 230 m depth and that there is no topographical trace of such a late displacement with a considerable vertical component, partly contradict the assumption that the sandstone in KSH03 is Cambrian. The deformation zone has most likely been active before the emplacement of the sandstone, as suggested by mylonites and extensive cataclasite formation of possible Meso-Proterozoic age. However, the cataclasite has probably been re-activated during the faulting that emplaced the sandstone at its present level. It should also be noted that although the sandstone is found in the deformation zone it may possibly have been emplaced through fractures outside the zone. Some speculative scenarios of the emplacement of the sandstone are briefly described below.

A scenario might involve reactivation of the pre-existing zone by movements. Re-activated fractures in the zone may be filled synchronously with sediments currently covering the bedrock surface. High fluid pressure in the sediments may even induce migration of fractures through hydraulic fracturing down to considerable depths in the already highly fractured zone, in accordance with /Röshoff and Cosgrove 2002/. They suggested that an advanced fluid pressure in sediments overlying the basement caused hydraulic fracturing in the basement and synchronous sediment infilling in the fractures, as an explanation for sediment filled fractures of presumed Cambrian age in the Götemar granite. This scenario involves un-consolidated sediments with high fluid pressures at the bottom of a relatively thick sedimentary pile. It is however difficult to determine how competent (consolidated or not) the sandstone was when it was emplaced in the deformation zone. The texture of the sandstone appears to be primary which contradicts a passive filling of loose sediments. Another scenario is that the sandstone was faulted down to its present level, possibly in a series of events.

Clastic sediments, of alleged lower Cambrian age, have been observed in thin fractures in tunnels on the Swedish west coast at levels of 50 m below the bedrock surface /Samuelsson 1975/. These fractures were filled by partly un-consolidated sediments synchronously with the fracturing. Continuous sediment filled fractures, extending down to more than 300 m below the bedrock surface, have been reported from other parts of the world cf /Röshoff and Cosgrove 2002/.

### *Sandstone occurrences nearby*

Other sandstone occurrences in southern Sweden are of Jotnian type, with an unconstrained age of 1,600 Ma /Gorbatshev and Gaal 1986/ to about 1,460 Ma /Söderlund et al. 2005/ for the lower part of the sedimentary succession. Jotnian sediments are found at several locations in Sweden, Finland and the Baltic Sea, e.g. in the Landsort Deep about 150 km to the northeast of the area /Flodén 1980/. 1,490–1,540 Ma old, possibly Jotnian sediments near the Landsort Deep (Gotska Sandön) are predominantly medium-grained, hard, grey to greenish- or yellowish-grey sandstone, locally containing clay matrix /Gorbatshev

1962/. Comparisons of the Gotska Sandön rock and Jotnian rocks like the Mälar and Gävle sandstone shows that the Gotska Sandön have lower amount of K-feldspar (3–11%, compared to 10–30% for Jotnian rocks), higher matrix content (4–35% compared to 0–10% for Jotnian rocks), less roundness (moderate, compared to good to moderate for Jotnian rocks), and lower amount of heavy minerals, although the sorting-grade of the sand is the same /Gorbatshev 1962/. The Jotnian sediments may have covered southern Sweden with a very extensive cover /Eichstädt 1885, Magnusson et al. 1963, Rodhe 1987/. Jotnian Dala sandstone and Gävle sandstone are commonly reddish but yellowish and whitish varieties also occur /Magnusson et al. 1963/.

Another sedimentary sequence is the Almesåkra group (about 120 km distance to the west), possibly of Sveconorwegian age as dolerites dated to 1,000 Ma /Patchett 1978/ intrudes consolidated but not completely cemented sediments cf /Rodhe 1985/. The Almesåkra group are composed largely of feldspathic arenitic sandstone, although minor occurrences of conglomerates and grey quartzitic sandstone are present /Rodhe 1987/. The Almesåkra sedimentary rocks are tectonically more disturbed and richer in argillites than Jotnian sequences /Rodhe 1987/. Generally, none of these sandstone occurrences fit the description of the KSH03-sandstone as good as the Cambrian sandstone does.

Another sandstone occurrence of southern Sweden is that of the Visingsö group (about 170 km distance to the WNW) deposited in a graben type basin, with an overall thickness of at least 1,000 m /Collini 1951/. The lower of the three units of the Visingsö Group is made up of very well sorted, medium-grained quartz sandstone or quartz arenite, the middle unit is characterised by reddish, greenish and greyish arkoses and graywackes, including shale and siltstone intercalations /Vidal 1974, Morad and Aldahan 1986/. Shale and siltstone of the Visingsö formation has been dated with Rb-Sr isotopes to 663–703 Ma and to 711–763 Ma with the K-Ar method. The lower age ( $663 \pm 7$  Ma) is interpreted to record the diagenetic event and thus a minimum age of the upper unit /Bonhomme and Welin 1983/. /Vidal et al. 1993/ considered the upper Visingsö Group to be of late Riphean age. Interestingly, relatively abundant Ti-oxides have been found in the Visingsö sediments /Morad and Aldahan 1986, Morad and Aldahan 1987/, a feature that is also observed in the sandstone of KSH03. The Visingsö sandstone is however generally quite K-feldspar-rich /Aldahan and Morad 1986/, as opposed to the sandstone in KSH03.

### *Conclusion*

As stated above the sandstone in KSH03 resembles Cambrian sandstone in colour, composition, sorting and roundness in contrast to the more K-feldspar-rich Jotnian sandstone, Almesåkra sandstone and Visingsö sandstone, although the K-feldspar content is locally low in these rocks as well. The sandstone from Gotska Sandön generally has a much higher amount of matrix than the sandstone in KSH03. In conclusion: The age and emplacement of the sandstone can not be discerned based on the information from this drill core observation. What can be concluded is that the deformation zone is older than the sandstone, that the sandstone probably is Cambrian and that emplacement of the sandstone in the deformation zone probably took place before  $405 \pm 27$  Ma.

## **7.3 Stable isotope studies of calcite**

The stable isotope results ( $\delta^{13}\text{C}$ ,  $\delta^{18}\text{O}$  and  $^{87}\text{Sr}/^{86}\text{Sr}$ ) are presented in the appendix. The analysed calcite samples are from different generations, based on cross-cutting relations and paragenesis.

### 7.3.1 $\delta^{13}\text{C}$ and $\delta^{18}\text{O}$

$\delta^{13}\text{C}$ - and  $\delta^{18}\text{O}$ -results show that the calcite samples are similar in isotopic composition to calcite of earlier studies in the area e.g. /Wallin and Peterman 1999, Bath et al. 2000, Tullborg 2000, Drake and Tullborg 2004, 2006a/. They also show that the calcite precipitated during several events with different, mostly hydrothermal conditions (low  $\delta^{18}\text{O}$ , relatively high  $\delta^{13}\text{C}$ , “3” in Figure 7-15) and at moderate temperatures (low  $\delta^{18}\text{O}$ , higher  $\delta^{13}\text{C}$ , “6” and “7” in Figure 7-15). Calcite samples of generation 5 give different isotopic signature (both hydrothermal and more moderate temperatures), which show that these fillings have precipitated at several events. Calcite in generation 6 mostly plot in “6” in Figure 7-15 ( $\delta^{13}\text{C} = -21$  to  $-10$  ‰,  $\delta^{18}\text{O} = -14$  to  $-9$  ‰) which is in accordance with scalenohedral calcite, precipitated from “warm brine”, in similar paragenesis from Simpevarp, Laxemar, Äspö and Götömar e.g. /Bath et al. 2000, Drake and Tullborg 2004, 2006a, in manuscript, Tullborg 2004/. Two samples plot in field “7” in Figure 7-15 and probably represent calcite of mixed origins possibly with younger low temperature components. Some of the calcite from samples that cut through the cataclasite has values that are similar to that of generation 3. The main cataclasite formation event might then be older than generation 3.

### 7.3.2 Sr-isotopes

The Sr isotope values in the six analysed fracture calcites range from about 0.707 to 0.722. A plot of Sr-isotope ratio versus  $\delta^{18}\text{O}$  values for fracture calcites in KSH03 and KSH01 /Drake and Tullborg 2004/ and KLX03, KLX04, KLX05, KLX06 /Drake and Tullborg, in manuscript/, KKR02, KKR03 /Drake and Tullborg 2006a/, KA1755A and KAS17 /Drake and Tullborg, unpublished data/ is shown in Figure 7-16. The sample with a Sr isotope ratio of 0.722 (“4” in the figure) is probably contaminated and is thus left out of the discussion.

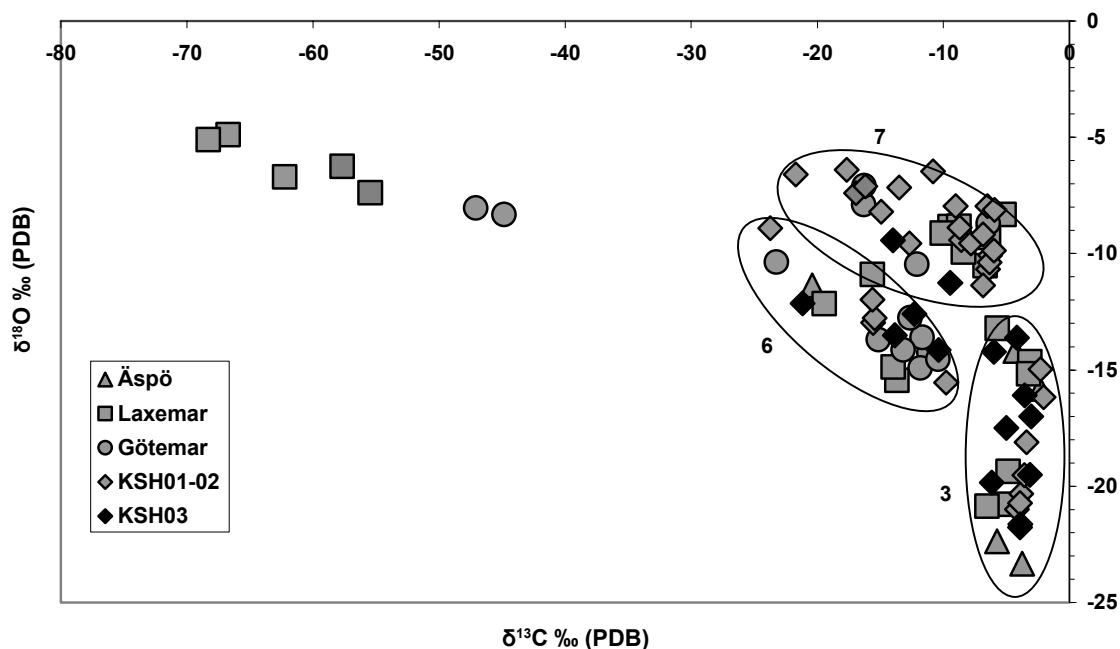


**Figure 7-15.**  $\delta^{13}\text{C}/\delta^{18}\text{O}$  values for fracture calcites in KSH03 plotted together with earlier analysed samples from KSH01, Simpevarp /Drake and Tullborg 2004/, KLX03, KLX04, KLX05, KLX06, Laxemar /Drake and Tullborg, in manuscript/, KKR02, KKR03, Götömar /Drake and Tullborg, 2006a/, KA1755A and KAS17 Äspö /Drake and Tullborg, unpublished data/. See text for details.

There is a general trend with higher  $^{87}\text{Sr}/^{86}\text{Sr}$  ratios in samples with higher  $\delta^{18}\text{O}$  values which is in agreement with earlier observations by /Wallin and Peterman 1999, Bath et al. 2000, Drake and Tullborg 2004/, showing the lowest  $^{87}\text{Sr}/^{86}\text{Sr}$  isotope ratios and the lowest  $\delta^{18}\text{O}$  values for the hydrothermal calcites. The  $^{87}\text{Sr}/^{86}\text{Sr}$ -ratios vary especially for calcite from generation 5 which ranges from 0.707 to 0.712, which further suggests that this generation should be divided into several generations (“1” to “3” in Figure 7-16). This also suggest that some laumontite is formed very early in the fracture filling sequence and that some laumontite is formed late in the sequence. Since all of the calcites analysed for Sr isotopic composition are found in fractures cutting through cataclasite it can be suggested that the major cataclasite formation took place early in the fracture filling sequence (earlier than generation 3) in correlation with other observations in this study.

Calcite from generation 6 shows a higher  $^{87}\text{Sr}/^{86}\text{Sr}$ -ratio (0.715) than calcite from earlier generations, which is in agreement with similar calcite samples from KSH01 (“3” in Figure 7-16) /Drake and Tullborg 2004/. The sample with  $^{87}\text{Sr}/^{86}\text{Sr}$ -ratio 0.712 may however be included in generation 6 as well. The Sr isotope ratios from generation 6 from Simpevarp are generally lower than in similar calcite from Laxemar, which in turn is generally lower than that in calcite from Götemar fracture fillings. Since these calcite fillings form Simpevarp, Laxemar and Götemar are thought to be coeval (see details above), the somewhat lower  $^{87}\text{Sr}/^{86}\text{Sr}$ -ratios in Simpevarp may reflect the wall rock chemistry, with generally lower K (and Rb) concentrations in Simpevarp than in Laxemar, which in turn has lower K (and Rb) concentrations than the Götemar granite. This is since higher Sr-ratios may reflect higher addition of  $^{87}\text{Sr}$  from wall rock that is richer in K (and Rb).

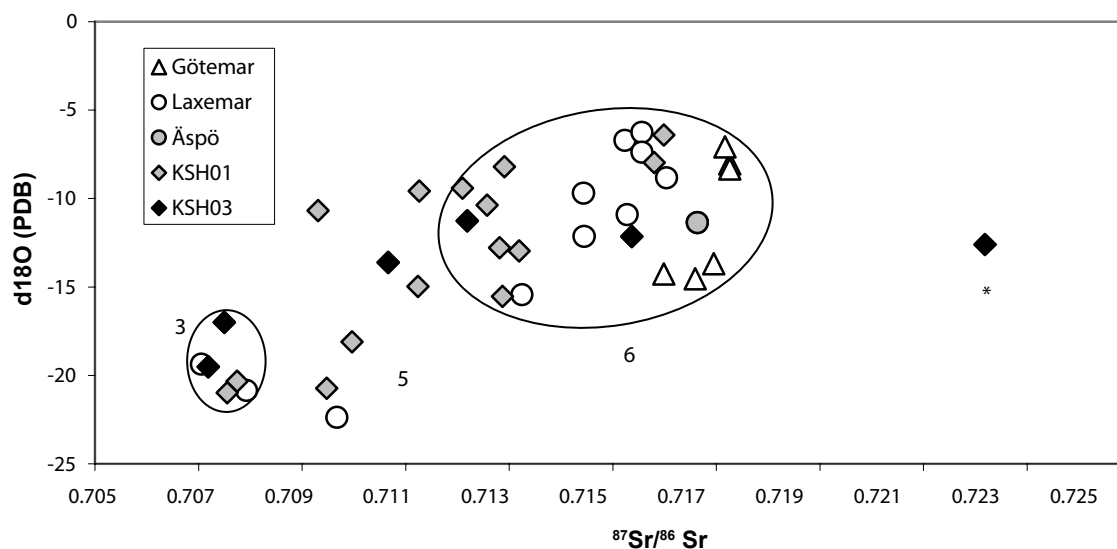


**Figure 7-16.** Sr isotope ratio plotted versus  $\delta^{18}\text{O}$  values for fracture calcites in KSH03 and KSH01 /Drake and Tullborg 2004/, KLX03, KLX04, KLX05, KLX06 /Drake and Tullborg, in manuscript/, KKR02, KKR03 /Drake and Tullborg 2006a/, KA1755A and KAS17 /Drake and Tullborg, unpublished data/. “3” is old hydrothermal calcite, “5” is somewhat younger calcite “6” is dominantly scalenohedral calcite of similar paragenesis and  $\delta^{13}\text{C}/\delta^{18}\text{O}$ -ratios and “\*” is a sample that might be contaminated.

## 8 Summary

The characteristics of the fracture fillings are fairly similar throughout the drill core although the deformation zone is more intensively fractured and re-activated than the surrounding rock.

The deformation zone show signs of re-activation during several events. A small part of the deformation zone is made up of mylonite, while the major part of the zone is made up of cataclasite cross-cut by later fractures filled with minerals of several generations, mainly calcite, adularia and chlorite. The cataclasite can be divided into some sub-generations of different colour and mineralogy, reflecting re-activation at different events. The major cataclasite formation is however interpreted to have taken place quite early. Subsequent fracture fillings can also be divided into several generations. The earliest formed fractures that cross-cut the cataclasite are filled with calcite, adularia, laumontite, quartz, chlorite, illite, hematite, and occasionally prehnite. Stable isotope results suggest that these fillings are formed at several events during a long time sequence with gradually lower formation temperatures.

A later formed, better established fracture filling generation consists of calcite, adularia, chlorite, hematite, fluorite, quartz, pyrite, barite, illite/chlorite (ML-clay), corrensite, and occasionally gypsum, REE-carbonate, apophyllite, chalcopyrite, galena, sphalerite, Ti-oxide, U-silicate, laumontite, Cu-oxide and apatite. The paragenesis and stable isotope results from this generation are in accordance with fracture fillings of presumed Palaeozoic age identified earlier in the area e.g. /Wallin and Peterman 1999, Bath et al. 2000, Drake and Tullborg 2004, 2005, 2006a, in manuscript, Sundblad et al. 2004, Tullborg 2004/. It is found in fractures cutting through the sandstone in the deformation zone. The sandstone is presumed to be of Cambrian age but the actual displacement of the sandstone to the present depth (about 230 m below the horizontal plane) has probably taken place later than the Cambrian.

## 9 Acknowledgements

We would like to thank the staff at the SKB site investigations at Simpevarp for their support. Owe Gustafsson at Earth Sciences Centre, Göteborg University carried out the O and C isotope analyses on calcite. Göran Åberg at Institute for Energy Technology, Norway carried out Sr isotope analyses on calcite. Sven Snäll at SGU carried out XRD analyses. Kjell Helge and Ali Firoozan have carried out thin section preparation. Sven Åke Larson, Göteborg University contributed with valuable comments to the manuscript. Herbert Henkel (KTH), Tom Flodén (Stockholm University), Piret Plink-Björklund (Göteborg University) and Carl-Henric Wahlgren (SGU) are thanked information about sandstones. Mikael Erlström, SGU, is thanked for the detailed investigation of the sandstone thin sections. Björn Sandström, Göteborg University, is thanked for providing references. Fredrik Hartz, SKB, kindly helped us with the map for the area.

## 10 References

- Aldahan A A, Morad S, 1986.** Mineralogy and chemistry of diagenetic clay minerals in Proterozoic sandstones from Sweden, *American Journal of Science*, 286, p 29–80.
- Alm E, Sundblad K, 2002.** Fluorite-calcite-galena-bearing fractures in the counties of Kalmar and Blekinge, Sweden. SKB R-02-42. 116 pp. Svensk Kärnbränslehantering AB.
- Bath A, Milodowski A, Ruotsalainen P, Tullborg E-L, Cortés Ruiz A, J-F A, 2000.** Evidences from mineralogy and geochemistry for the evolution of groundwater systems during the quaternary for use in radioactive waste repository safety assessment (EQUIP project). EUR report 19613.
- Bonhomme M G, Welin E, 1983.** Rb-Sr and K-Ar isotopic data on shale and siltstone from the Visingsö Group, Lake Vättern Basin, Sweden, *Geologiska Föreningen i Stockholm Förhandlingar*, 105, p 363–366.
- Collini B, 1951.** Visingsöformationen, In *Beskrivning till kartbladet Gränna, Sveriges Geologiska Undersökning*, Aa 193, p 22–37.
- Drake H, Tullborg E-L, 2004.** Fracture mineralogy and wall rock alteration, results from drill core KSH01A+B. SKB P-04-250. 120 pp. Svensk Kärnbränslehantering AB.
- Drake H, Tullborg E-L, 2005.** Fracture mineralogy and wall rock alteration, results from drill cores KAS04, KA1755A and KLX02. SKB P-05-174. 69 pp. Svensk Kärnbränslehantering AB.
- Drake H, Tullborg E-L, 2006a.** Fracture mineralogy of the Götemar granite, Results from drill cores KKR01, KKR02 and KKR03. SKB P-06-04. Svensk Kärnbränslehantering AB, submitted to SKB.
- Drake H, Tullborg E-L, 2006b.** Mineralogical, chemical and redox features of red-staining adjacent to fractures, Results from drill cores KSH01A+B and KSH03A+B. SKB P-06-01. Svensk Kärnbränslehantering AB, Submitted to SKB.
- Drake H, Tullborg E-L, in manuscript.** Fracture mineralogy, results from drill cores KLX03, KLX04, KLX05, KLX06, KLX07A+B, KLX08, and KLX10A. P-XX-XX. Svensk Kärnbränslehantering AB.
- Drake H, Tullborg E-L, unpublished data.** Fracture mineralogy investigations of drill cores KA1755A, and KAS17. Svensk Kärnbränslehantering AB.
- Drever S I, 1973.** The preparation of oriented clay mineral specimens for X-ray diffraction analysis by a filter-membrane peel technique. *American Mineralogist*, 58, p 553–554.
- Ehrenborg J, Stejskal V, 2004.** Boremap mapping of core drilled boreholes KSH03A and KSH03B. Oskarshamn site investigation. SKB P-04-132. 24 pp. Svensk Kärnbränslehantering AB.
- Eichstädt, 1885.** Om kvartsit-diabaskonglomeratet i Småland och Skåne, *GFF*, VII, p 610–630.



- Flodén T, 1980.** Seismic stratigraphy and bedrock geology of the central Baltic, Stockholm contributions in geology, Vol. 35, p 240.
- Gaal G, Gorbatshev R, 1987.** An outline of the Precambrian evolution of the Baltic Shield. In: 1987, Precambrian geology and evolution of the central Baltic Shield; 1st Symposium on the Baltic Shield. 35. p 15–52. Elsevier, Amsterdam, International
- Gorbatshev R, 1962.** The Pre-Cambrian sandstone of the Gotska Sandön boring core. Bulletin of the Geological Institutions of the University of Uppsala, New Series, 39, p 1–30.
- Gorbatshev R, Gaal G, 1986.** The Precambrian history of the Baltic Shield. In: A. Kröner, ed.: “Proterozoic Litospheric Evolution”. American Geophys. Union, Geodynamic Series.
- Hessland I, 1955.** Studies in the lithogenesis of the Cambrian and basal Ordovician of the Böda Hamn sequence of strata, Bull. of the Geol. Instit. of Uppsala, Vol 35, p 109.
- Hultgren P, Stanfors R, Wahlgren C-H, Carlsten S, Mattsson H, 2004.** Geological single-hole interpretation of KSH03A, KSH03B, KLX02, HAV09 and HAV10. Oskarshamn site investigation. SKB P-04-231. 37 pp. Svensk Kärnbränslehantering AB.
- Kornfält K A, Wikman H, 1987.** Description of the map of solid rocks around Simpevarp. SKB PR-25-87-02. 45 pp. Svensk Kärnbränslehantering AB.
- Kornfält K A, Persson P O, Wikman H, 1997.** Granitoids from the Äspo area, southeastern Sweden; geochemical and geochronological data, Gff, 119, p 109–114.
- Kresten P, Chyssler J, 1976.** The Götemar Massif in south-eastern Sweden; a reconnaissance survey, Geologiska Föreningen i Stockholm Förhandlingar, 98, Part 2, p 155–161.
- Larson S Å, Berglund J, 1992.** A chronological subdivision of the Transscandinavian igneous belt three magmatic episodes? Geologiska Föreningen i Stockholm Förhandlingar, p 459–461.
- Lindström M, 1991.** Den yngre berggrunden. In: Lindström M, Lundqvist J, and Lundqvist T, 1991, Sveriges geologi från urtid till nutid. p 123–230. Studentlitteratur, Lund
- Maddock R H, Hailwood E A, Rhodes E J, Muir Wood R, 1993.** Direct fault dating trials at the Äspö Hard Rock Laboratory. SKB TR-93-24. 189 pp. Svensk Kärnbränslehantering AB.
- Magnusson N H, Lundqvist G, Regnéll G, 1963.** Sveriges geologi, 4:e uppl. Svenska Bokförlaget, Norstedts. Stockholm, 698 pp.
- Milodowski A E, Tullborg E-L, Buil B, Gomez P, Turrero M-J, Haszeldine S, England G, Gillespie M R, Torres T, Ortiz J E, Zacharias, Silar J, Chvatal M, Strnad L, Sebek O, Bouch, Jesr Chenery1 C, Chenery C, Sheperd T J, 2005.** Application of mineralogical, Petrological and Geochemical tools for Evaluating the Palaeohydrogeological Evolution of the PADAMOT Study Sites. PADAMOT Project Technical Report WP2.
- Morad S, and Aldahan A A, 1986.** Alteration of detrital Fe-Ti oxides in sedimentary rocks, Geological Society of America Bulletin, 97, p 567–578.
- Morad S, and Aldahan A A, 1987.** Diagenetic “replacement” of feldspars by titanium oxides in sandstones, Sedimentary Geology, 51, p 147–153.
- Patchett P J, 1978.** Rb/Sr ages of Precambrian dolerites and syenites in South and Central Sweden, SGU C747, p 1–63.

**PDF, 1994.** Powder diffraction file computer data base. International Centre for Diffraction Data, Park Lane, Swartmore, PA, USA. p 1–43.

**Rodhe A, 1985.** Geochemistry and clay mineralogy of argillites in the late Proterozoic Almesåkra Group, South Sweden, Geologiska Föreningen i Stockholm Förhandlingar, 107, p 175–182.

**Rodhe A, 1987.** Depositional environments and lithostratigraphy of the middle Proterozoic Almesåkra Group, southern Sweden. Sveriges Geologiska Undersökning, Serie Ca: Avhandlingar och Uppsatser i 4:o. Lund Publications in Geology, Vol. 73, Sveriges Geologiska Undersökning. Uppsala, Sweden, 80 pp.

**Röshoff K, Cosgrove J, 2002.** Sedimentary dykes in the Oskarshamn-Västervik area – A study of the mechanism of formation. SKB R-02-37. 98 pp. Svensk Kärnbränslehantering AB.

**Samuelsson L, 1975.** Palaeozoic fissure fillings and tectonism of the Göteborg area, south-western Sweden. Sveriges Geologiska Undersökning, Serie C, Avhandlingar och uppsatser, Nr 711, Årsbok 69, Nr 3, 43 pp.

**Sundblad K, Alm E, Huhma H, Vaasjoki M, Sollien D B, 2004.** Early Devonian tectonic and hydrothermal activity in the Fennoscandian Shield; evidence from calcite-fluorite-galena mineralization, In: Mertanen S (ed), Extended abstracts, 5th Nordic Paleomagnetic workshop. -Supercontinents, remagnetizations and geomagnetic modelling, Geological Survey of Finland, p 67–71.

**Söderlund U, Isachsen C E, Bylund G, Heaman L M, Patchett P J, Vervoort J D, Andersson U B, 2005.** U-Pb baddeleyite ages and Hf, Nd isotope chemistry constraining repeated mafic magmatism in the Fennoscandian Shield from 1.6 to 0.9 Ga, Contrib. Mineral Petrol, vol. 150, p 174–194.

**Tullborg E-L, 1988.** Fracture fillings in the drillcores from Äspö and Laxemar. In: **Wikman H, Kornfält K-A, Riad L, Munier R, Tullborg E-L, 1988.** Detailed investigations of the drillcores KAS02, KAS03 and KAS04 on Äspö Island and KLX01 at Laxemar. SKB PR 25-88-11. 30 pp. Svensk Kärnbränslehantering AB.

**Tullborg E-L, 1995.** Chapter 4. Mineralogical/Geochemical Investigations in the Fracture Zone. In: Banwart S, 1995, The Redox experiment in block scale. SKB PR 25-95-06. p 81–101.

**Tullborg E-L, 1997.** Recognition of low-temperature processes in the Fennoscandian Shield: Doctoral thesis, Earth Science Centre A17, Göteborg University, 35 pp.

**Tullborg E-L, 2000.** Ancient microbial activity in crystalline bedrock; results from stable isotope analyses of fracture calcites. In, 2000, Hydrogeology of crystalline rocks. 34. p 261–275. Kluwer Academic Publishers, Dordrecht, Netherlands

**Tullborg E-L, 2004.** Palaeohydrogeological evidences from fracture filling minerals\_ Results from the Äspö/Laxemar area, Mat. Res.Soc. Symp. Vol 807, p 873–878.

**Wahlgren C-H, Ahl M, Sandahl K-A, Berglund J, Petersson J, Ekström M, Persson P-O, 2004.** Bedrock mapping 2003 – Simpevarp subarea. Outcrop data, fracture data, modal and geochemical classification of rock types, bedrock map, radiometric dating. Oskarshamn site investigation. SKB P-04-102. 59 pp. Svensk Kärnbränslehantering AB.

**Wallin B, Peterman Z, 1999.** Calcite fracture fillings as indicators of palaeohydrogeology at Laxemar at the Äspö Hard Rock Laboratory, southern Sweden. *Applied Geochemistry*, Vol. 14, p 953–962.

**Vidal G, 1974.** Late Precambrian microfossils from the basal sandstone unit of the Visingsöe Beds, South Sweden, *Geologica et Palaeontologica*, 8, p 1–14.

**Vidal G, Moczydlowska M, Rudavskaya V A, 1993.** Biostratigraphical implications of a Chuaria-Tawuia assemblage and associated acritarchs from the Neoproterozoic of Yakutia, *Palaeontology*, 36, p 387–402.

**Åberg G, Löfvendahl R, Levi B, 1984.** The Göttemar granite-isotopic and geochemical evidence for a complex history of an orogenic granite, *Geologiska Föreningen i Stockholm Förhandlingar*, 106, p 327–333.

**Åhäll K-I, 2001.** Åldersbestämning av svårdaterade bergarter i sydöstra Sverige. SKB R-01-60. 28 pp. Svensk Kärnbränslehantering AB.

**Åhäll K I, Larson S Å, 2000.** Growth-related 1.85–1.55 Ga magmatism in the Baltic Shield; a review addressing the tectonic characteristics of Svecofennian, TIB 1-related, and Gothian events, *GFF*, 122, p 193–206.

### A1 Sample descriptions

“n.d.” = below the detection limit for SEM-EDS.

#### ***KSH03B: 14.97–15.32 m (1)***

Sample type: Thin section.

Rock type: Quartz monzodiorite.

Fracture: Network of mainly 2 mm wide sealed fractures. The fractures are coated by a red to brick red fracture filling with white to yellowish grey coloured feldspar and calcite filling in the middle of the fractures. There are two preferred orientations of the fractures, one is cutting the drill core with an angle of 45° (279/16°), and the other is cutting the drill core perpendicularly. The fractures are filled with the same paragenetic minerals, which indicate that the fractures are coeval.

Minerals: Adularia, calcite and hematite.

The minerals in this filling appear to be formed at a single event. Adularia is the most common mineral and is often coating the fracture walls. Calcite is found in the centre of the sealed fracture. Hematite crystals are found in between crystals of adularia.

Wall rock alteration: Intensely red coloured wall rock due to oxidation, mainly affecting the plagioclase crystals, which are completely replaced by secondary minerals, mainly albite and K-feldspar. Biotite is completely replaced by chlorite. The wall rock is highly porous.



*Photograph of drill core sample 14.97–15.32 m (1) with fractures filled with adularia (arrow), calcite and hematite (red). Drill core diameter is about 50 mm.*

**KSH03B: 14.97–15.32 m (2)**

Sample type: X-Ray Diffraction.

Rock type: Quartz monzodiorite.

Fracture: Sealed fracture (3 cm wide) filled with mainly clinocllore (Mg-rich chlorite).

**KSH03A: 111.80–111.92 m**

Sample type: Thin section.

Rock type: Ävrö Granite, weakly oxidized.

Fracture: Two different fracture sets, each represented by numerous 1 mm wide sealed fractures with wall rock in between, are dominating a 5–10 wide zone of intense fracturing. A green, epidote-dominated filling seals the earliest formed fracture set. The younger fracture (214/60°) set is filled with a reddish brown filling. Both of these fracture networks are cut by a millimetre wide fracture filled with calcite and adularia. The fracture networks appear to be thin cataclasites that have been re-activated on more than one occasion.

Minerals: Calcite, adularia, chlorite, epidote, hematite, barite, illite (ML-clay), prehnite, fluorite and Cu-oxide.

1. Cataclasite with a high content of angular epidote crystals and adularia crystals. Often very fine-grained and dark coloured.
2. Cataclasite with a higher content of Mg-rich chlorite and a lower content of epidote than in “generation 1”. This filling mainly consists of adularia and is also more hematite-rich and more reddish in colour than in “generation 1”.
3. Calcite ( $\text{MnO}_2 = \text{n.d. to } 0.7\%$ ) filled fractures bordered by euhedral adularia and prehnite. Sometimes the adularia fills the whole fracture and some times calcite is merely visible as small crystals in the middle of the filling. Mg-rich chlorite is sometimes bordering these fillings and is thought to be coeval with quartz and adularia. Hematite crystals ( $< 5 \mu\text{m}$ ) are sometimes present in the adularia-rich parts of the filling.
4. Thin fractures (20–40  $\mu\text{m}$  wide) are cutting the calcite/adularia fillings perpendicularly. These fractures are filled with calcite ( $\text{MnO}_2 = 0.15\text{--}0.25\%$ ) with very small amount of fluid inclusions and deformational twin-lamellae together with fluorite and small crystals of barite and Cu-oxide (Ni-Zn-rich). Some illite in mixed layer clay with chlorite may be present in paragenesis with calcite (few observations).

Fillings made up of prehnite with adularia (presumably formed later) are cutting through cataclasite of generation 1. There are few relations between prehnite and cataclasite of generation 2 but fragments of prehnite are present in the cataclasite of generation 2 at one location.

Wall rock alteration: High degree of micro-fracturing. Secondary minerals like epidote and chlorite are abundant. Primary plagioclase is completely replaced by e.g. albite and K-feldspar, in a pseudomorphic manner. The pseudomorphs are red-stained. Polycrystalline, fine-grained quartz crystals and fine-grained secondary minerals are abundant in between bigger feldspar crystals.



*Photograph of drill core sample 111.80–111.92 m with fractures filled with calcite and adularia (white), cross-cutting epidote-rich cataclasite (green) and hematite-rich cataclasite (red). Drill core diameter is about 50 mm.*

**KSH03A: 117.75–117.94 m**

Rock type: Quartz monzodiorite, faintly oxidized.

Fracture: Open fracture (133/03°, 6.0 mm wide), coated with red-brown gouge material.

Minerals according to X-ray diffraction: Quartz, K-feldspar, calcite, hematite, corrensite and clinocllore (Mg-rich chlorite).



*Photograph of drill core sample 117.75–117.94 m with the gouge-coated open fracture sampled for XRD-analysis in the middle of the photo. Drill core diameter is about 50 mm.*

**KSH03A: 126.00–126.22 m (1)**

Sample type: Thin section.

Rock type: Quartz monzodiorite, faintly oxidized.

Fracture: A one centimetre wide, brown to reddish brown filling is cut by a < 1 mm wide fracture filled with brightly coloured minerals (240/57°). This fracture offsets the earlier formed fracture.

Minerals: Adularia, calcite, illite, chlorite, and hematite.

Order of fracture fillings:

1. Two varieties of hematite-rich fillings can be identified in this sample. The major brown to reddish brown filling consists of adularia, Mg-rich chlorite, Fe-rich chlorite and hematite, in order of abundance. This filling also contains some larger fragment of K-feldspar, possibly from the wall rock. Some parts of this filling are more hematite rich and less rich in chlorite. The second variety of the hematite rich filling is mostly parallel to the fracture of next generation. This hematite-rich filling consists of adularia, Mg-rich chlorite and hematite and may be formed later than the first described variety.
2. Calcite, adularia and illite. The calcite has an undetectable (SEM-EDS) amount of MnO<sub>2</sub>. This filling is sealing the fracture that is cutting through the hematite-cataclasite.

Wall rock alteration: High degree of alteration and micro-fracturing.



*Photograph of drill core sample 126.00–126.22 m with a fracture filled with calcite, adularia and illite (bright), cross-cutting hematite-rich cataclasite (reddish brown). Lines show the position of the thin section. Drill core diameter is about 50 mm.*

**KSH03A: 126.00–126.22 m (2)**

Sample type: Thin section.

Rock type: Quartz monzodiorite, faintly oxidised.

Fracture: A one centimetre wide, brown to reddish brown filling is cut by a < 1 mm wide fracture (221/58°). The reddish brown filling is also present in several fractures, together forming a fracture network through the drill core sample.

Minerals: Adularia, calcite, laumontite, chlorite, hematite, prehnite, and small amounts of epidote, barite, galena and apatite.

Order of fracture fillings:

1. Euhedral and partly dissolved prehnite crystals. The prehnite is filling fractures that cut and offsetting earlier formed fine-grained fillings. These fillings seem to be epidote-rich and some parts may be enriched in hematite as well.
2. Cataclastic filling consisting of small amounts of hematite, adularia, chlorite and some small crystals of titanite.
3. Filling consisting of laumontite, adularia, hematite, calcite ( $\text{MnO}_2 = \text{n.d.}$ ) and Fe-rich chlorite is cutting through the earlier formed cataclasite perpendicularly. Adularia and laumontite are the most abundant minerals in this filling and the crystals are often euhedral. The Fe-rich chlorite ( $\text{FeO} = 36\%$ ,  $\text{MgO} = 6\%$ ) is present on the outermost surface of this filling and is also present in voids in between euhedral adularia crystals. This might indicate that the Fe-rich chlorite is formed later than the other minerals in this filling. Small amounts of barite, galena and apatite are present along with Fe-rich chlorite.

Wall rock alteration: High degree of alteration and micro-fracturing.

**KSH03A: 177.74–177.81 m (1)**

Sample type: Thin section.

Rock type: Quartz monzodiorite, faintly oxidized.

Fracture: The sample consists of re-activated fractures of several generations, filled with e.g. quartz, hematite-cataclasite, calcite and laumontite. The fracture fillings are generally about 5 mm wide but the laumontite-dominated fillings are wider. The thin section displays dominantly 5 mm wide fillings of quartz (224/87°), calcite (224/70°) and a centimetre wide laumontite/adularia/calcite filling.

Minerals: Quartz, calcite, adularia, laumontite, chlorite, epidote, titanite, barite, hematite and small amounts of galena, pyrite, sphalerite and Cu-oxide.

Order of fracture fillings:

1. Epidote-rich cataclasite with small amounts of titanite and K-feldspar.
2. Quartz filling in e.g. a millimetre-wide fracture. This fracture is hard to relate to the epidote-cataclasite but is evidently older than the fractures of generation “2”.
3. Laumontite – adularia – calcite ( $\text{MnO}_2 = \text{n.d.}$ ) – hematite – Mg-rich chlorite. Calcite is formed later than laumontite and adularia and these three minerals are occupying most of the thin section. Especially laumontite and adularia are abundant in one part of the sample and calcite bordered by some adularia and laumontite is present in a millimetre



wide homogeneous filling. This calcite host more twin lamellae and fluid inclusions, than the calcite of generation “4” in this thin section. Some of the calcite shows a high degree twinning and may be formed earlier than the laumontite.

4. Thin veins filled with calcite ( $\text{MnO}_2 < 1\%$ , few fluid inclusions), fluorite and small amounts of adularia and fine-grained barite (Sr-rich, about  $10\ \mu\text{m}$  big crystals), hematite, Fe-rich chlorite ( $\text{FeO} = 36\%$ ,  $\text{MgO} = 5.5\%$ ), euhedral pyrite (and galena, Cu-oxide [Pb-Zn-rich] and sphalerite).



*Photograph of drill core sample 177.74–177.81 m. Drill core diameter is about 50 mm.*

**KSH03A: 177.74–177.81 m (2)**

Sample type: Thin section.

Rock type: Quartz monzodiorite, faintly oxidized.

Fracture: The sample consists of re-activated fractures of several generations, filled with quartz, hematite-cataclasite, calcite, laumontite etc. The fillings are generally about 5 mm wide but the laumontite-dominated fillings are wider. This thin section mainly displays a calcite-laumontite-adularia filling and some thin calcite filled fractures.

Minerals: Calcite, adularia, laumontite, prehnite, chlorite, hematite, pyrite and epidote.

Order of fracture fillings:

1. Euhedral and partly dissolved prehnite crystals are present in later formed calcite.
2. Euhedral laumontite, adularia, calcite ( $\text{MnO}_2 = \text{n.d.}$ ) and anhedral hematite is dominant in this filling, the most abundant filling in this thin section. The filling is red to orange coloured due to the presence of hematite-stained laumontite and adularia. Some (possibly older) epidote, Fe-rich chlorite and Mg-rich chlorite ( $\text{FeO} = 4\%$ ,  $\text{MgO} = 26\%$ ) are present in small amounts of this filling.
3. Calcite ( $\text{MnO}_2 = < 1\%$ ) and pyrite is present in thin fractures through the earlier formed fillings.

Epidote-rich mylonite/cataclasite is present but is difficult to relate to other generations but it is evidently older than “generation 2”.

**KSH03A: 181.93–181.98 m**

Sample type: Thin section.

Rock type: Quartz monzodiorite, faintly oxidized.

Fracture:

1. About 4 cm wide, laumontite dominated fracture filling with minor calcite and feldspar (196/46°).
2. About 1 cm wide hematite-rich cataclasite cut by calcite (198/39°).

Minerals: Calcite, laumontite, quartz, adularia, hematite, epidote, apatite and chlorite.

Order of fracture fillings:

Fracture 1:

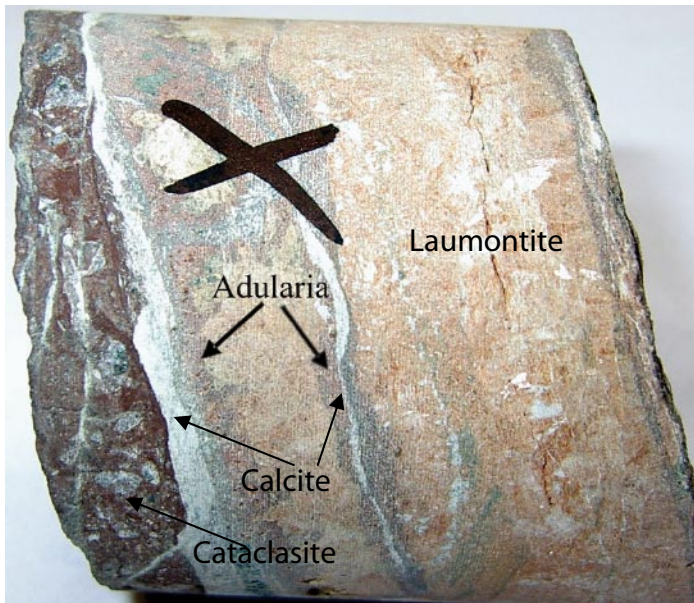
1. Calcite ( $\text{MnO}_2 = \text{n.d.}$ ) and adularia filling with numerous small voids, within crystals and in between crystals. Hematite crystals are sometimes present in these voids.
2. Laumontite and subordinate calcite ( $\text{MnO}_2 = \text{n.d.}$ ).

The fillings in “Fracture 1” may be slightly coeval since they are penetrating each other. Some Fe-rich chlorite ( $\text{FeO} = 43\%$ ,  $\text{MgO} = 2.5\%$ ) is also present along with laumontite.

Fracture 2:

1. Hematite-cataclasite consisting of fine-grained hematite and bigger grains of K-feldspar and quartz. Small grains of epidote and titanite are also present.
2. The hematite-cataclasite is cut by a fracture filled with calcite ( $\text{MnO}_2 = \text{n.d.}$ ). Earlier formed quartz is coating the fracture wall. Also present is adularia and apatite as well as minor amounts of hematite and quartz within the calcite filling.

Wall rock alteration: High degree of alteration. Primary plagioclase is completely replaced by e.g. albite and K-feldspar, in a pseudomorphic manner and biotite is completely replaced by chlorite. The pseudomorphs after primary plagioclase are red-stained.



*Photograph of drill core sample 181.93–181.98 m showing fracture fillings consisting of cataclasite, calcite, adularia and laumontite. Drill core diameter is about 50 mm.*

**KSH03A: 186.52–186.62 m**

Sample type: Thin section (100 µm thick).

Rock type: Quartz monzodiorite, medium oxidised.

Fracture: A 1–5 cm wide dark green fracture filling (78/9°) is cut and offset by two < 1 cm wide fractures filled with calcite and adularia. One of these two calcite filled fractures is displayed in the thin section (164/44°).

Minerals: Calcite, illite (ML-clay with chlorite), adularia, chlorite, quartz, hematite and small amounts of barite, REE-carbonate and Pb/Y-silicate.

Order of fracture fillings:

1. Green filling: Illite (possibly in mixed layer clay with chlorite) is dominant. Small crystals of hematite or Fe-stained illite are also present along with some fragments of Fe-Mg-chlorite and quartz.
2. Calcite ( $\text{MnO}_2 = 0.6\text{--}1.1\%$ ) with small amounts of hematite, quartz, barite, REE-carbonate and Pb/Y-rich silicate. The calcite filling is bordered by adularia.



*Photograph of drill core sample 186.52–186.62 m with fractures mainly filled with illite (green) and calcite (white). Drill core diameter is about 50 mm.*

**KSH03A: 197.79–197.85 m**

Sample type: Thin section.

Rock type: Fine-grained granite.

Fracture: A centimetre wide fracture filling is bordering a presently open fracture (244/56°). The fracture filling is made up of fillings of different generations starting from the wall rock with a 5 mm wide dark, reddish brown filling. This filling has dark green-coloured varieties that might be older. The outermost part of the coating consists of four millimetre wide fractures cutting through the dark reddish brown filling. These four fractures are filled with mainly calcite, adularia and laumontite.

Minerals: Calcite, adularia, chlorite, epidote, titanite, laumontite, quartz, illite, hematite and small amounts of muscovite and albite.

Order of fracture fillings:

1. Epidote-rich cataclasite, often with Fe-Mg-chlorite, titanite (both as individual anhedral grains and within chlorite crystals) and some muscovite.
2. Re-activation of cataclasite by fine-grained illite (mixed layer-clay), Mg-rich chlorite (FeO = 7%, MgO = 16%) and hematite. This filling might be coeval with “generation 3” in this sample.
3. Calcite ( $\text{MnO}_2 = \text{n.d.}$ ) in several parallel fractures with coeval quartz and adularia in between.
4. Calcite ( $\text{MnO}_2 = 1.3\text{--}2.96\%$ ) in a thin fracture coated by euhedral adularia. Laumontite is occasionally found in association with this filling

Notable: The cataclasites are very complex from re-activation and are thus hard to characterise properly in this thin section.

Wall rock alteration: Texturally unaffected. Primary plagioclase is completely replaced by e.g. albite and K-feldspar, in a pseudomorphic manner. Primary plagioclase twinning is occasionally preserved in the pseudomorphs. The pseudomorphs after primary plagioclase are red-stained. Most of the biotite is replaced by chlorite.

### ***KSH03A: 220.15–220.31 m***

Sample type: Thin section.

Rock type: Quartz monzodiorite, faintly oxidized.

Fracture: A fracture filled with a brown coloured, fine-grained filling is cut by a 5 mm wide fracture ( $198/11^\circ$ ), filled with dominantly calcite.

Minerals: calcite, hematite, adularia, albite, barite, chlorite, illite, epidote, quartz, REE-carbonate, Ti-oxide, pyrite and small amounts of galena and chalcopyrite.

Order of fracture fillings:

1. Brown-coloured cataclasite consisting of K-feldspar (adularia), Mg-rich chlorite (MgO = 17%, FeO = 12%) and hematite. Some quartz, albite and fine-grained epidote are also present.
2. Calcite ( $\text{MnO}_2 = \text{n.d.}$ ) in several pulses as elongated crystals, parallel to the fracture wall. Adularia crystals are found along the grain boundaries of the calcite crystals as well as on the fracture rim. Hematite is also present in between crystals of adularia and calcite. Some hematite crystals are penetrating through crystals of adularia and quartz. A thin fracture filled with calcite ( $\text{MnO}_2 = \text{n.d.}$ ) is cutting through the hematite filling which shows that these fillings are fairly coeval.
3. A thin vein of calcite and adularia coated by illite is cutting through the earlier formed fillings. Some Fe-rich chlorite, barite, REE-carbonate, Ti-oxide, pyrite, galena, and chalcopyrite are also present in this filling.



*Photograph of drill core sample 220.15–220.31 m showing brown cataclasite that is cut by fractures filled with e.g. calcite and adularia (bright). Drill core diameter is about 50 mm.*

**KSH03A: 225.44–225.49 m**

Sample type: Thin section.

Rock type: Quartz monzodiorite, faintly oxidized.

Fracture: A 3 mm wide fracture filling (230/17°) borders to a presently open fracture (230/19°, 2 mm wide). The fracture filling is made up of fillings of different generations which each are < 1 mm thick. The filling is porous in the contact zone towards the wall rock where several voids are visible.

Minerals: Quartz, calcite, adularia, chlorite, hematite, illite, REE-carbonate, muscovite, Ti-oxide and small amounts of apatite and barite.

Order of fracture fillings:

1. Red to brown coloured cataclasite (“hematite-cataclasite”) consisting of adularia, quartz, Fe-rich chlorite, Mg-rich chlorite and some hematite.
2. Quartz fills a fracture that cuts through the “hematite-cataclasite”
3. Mg-rich chlorite, calcite ( $\text{MnO}_2 = 0.5\%$ ) and rarely apatite is cutting through the quartz filling. The outermost filling in this sample consists of calcite ( $\text{MnO}_2 = 0.8\text{--}1.4\%$ ), adularia, REE-carbonate, Ti-oxide, illite and additional Fe-rich chlorite and barite. This filling is coeval with the filling of Mg-rich chlorite and calcite (+ apatite).

Muscovite is present along with adularia and Mg-chlorite of generation 3. It might however be fragments of earlier formed fillings.

Wall rock alteration: Texturally and structurally unaffected. Primary plagioclase is completely replaced by e.g. albite and K-feldspar, in a pseudomorphic manner. Primary plagioclase twinning is occasionally preserved in the pseudomorphs. The pseudomorphs after primary plagioclase are red-stained. Biotite is completely replaced by chlorite.

**KSH03A: 233.56–233.67 m**

Sample type: Thin section.

Rock type: Ävrö granite, faintly oxidized.

Fracture: Red/brown-coloured gouge filling (208/80°) borders and partly penetrates an older coarse-grained quartz filling (30/88°). The quartz filling is about 1–2 cm wide and the gouge filling is about 3–4 cm wide.

Minerals: Quartz, chlorite, hematite, adularia, clay minerals, calcite, albite, fluorite and small amounts of muscovite.

Order of fracture fillings:

1. Coarse-grained quartz, both as an individual filling and as fragments, in the later formed gouge filling. Some muscovite is found together with quartz fragments in the gouge filling.
2. Adularia is present in fractures cutting through the quartz filling.
3. Fine-grained gouge made up of Fe-rich chlorite (FeO = 31–46%, MgO = 3–6%), hematite and some clay minerals in association with chlorite. Adularia, calcite, fluorite, clay minerals, Fe-rich chlorite and albite are found in fractures cutting through the gouge. Quartz fragments of both rounded and angular shape are abundant in the gouge. Fe-rich chlorite is also penetrating through the quartz-filling.

**KSH03A: 245.03–245.07 m**

Sample type: Thin section.

Rock type: Quartz monzodiorite, faintly oxidized.

Fracture: A 5 mm thick brown to reddish brown fracture filling (129/25°) is re-activated by a fracture (126/28°, < 2 mm thick) filled with a greenish white filling.

Minerals: Adularia, chlorite, illite, hematite, calcite and small amounts of galena, sphalerite, corrensite and apatite.

Order of fracture fillings:

1. Hematite-cataclasite consisting of adularia, Mg-rich chlorite (FeO = 8–10%, MgO = 14–15%) and hematite, in order of abundance.
2. Adularia, illite and some calcite are filling fractures cutting the hematite-cataclasite. Very few hematite crystals and fragments of hematite are also present in this filling.
3. Fe-rich chlorite is present in micro-fractures cutting through the earlier formed fillings. Galena, sphalerite, corrensite and apatite are found in small amounts in relation to Fe-rich chlorite and calcite.

Wall rock alteration: Texturally unaffected. Primary plagioclase is completely replaced by e.g. albite and K-feldspar, in a pseudomorphic manner. Primary plagioclase twinning is occasionally preserved in the pseudomorphs. The pseudomorphs after primary plagioclase are red-stained. High degree of micro-fractures filled with hematite and/or Fe-oxyhydroxide cut through e.g. pseudomorphs after plagioclase.



Photograph of drill core sample 245.03–245.07 m showing dark brown hematite-cataclasite that is cut by a fracture filled with e.g. adularia, calcite, illite and chlorite. Drill core diameter is about 50 mm.

**KSH03A: 269.77–269.94 m**

Sample type: Thin section.

Rock type: Ävrö granite, medium oxidized.

Fracture: 1 cm wide fracture filled with a dark brown, fine-grained, filling (upper rim 166/51°, lower rim 169/51°).

The whole thin section consists of a fracture filling from one single generation. The filling consists of fine-grained, altered wall rock with no distinct preferred orientation of the minerals. Visible in hand sample is that this fracture filling probably is related to the “hematite-cataclasite” (see e.g. KSH03: 220.15–220.31 m). The “hematite-cataclasite”-part of the sample is however not included in the thin section.

Minerals: K-feldspar, chlorite, quartz, Fe-oxide, muscovite, apatite, albite and Ti-oxide.

K-feldspar, quartz and chlorite are the most abundant minerals.



Photograph of drill core sample 269.77–269.94 m. Drill core diameter is about 50 mm.

***KSH03A: 271.53–271.63 m (I)***

Sample type: Thin section.

Rock type: Sandstone and cataclasite.

Fracture: This sandstone occurrence has a total width of 37 cm, with a 2 cm wide, cross-cutting cataclasite/gouge-filling dividing the sandstone into two parts; 29 cm and 8 cm, respectively. The sandstone is bordered by red-coloured cataclasite/gouge-material on both sides in the drill core. The sampled part of the sandstone borders to the cataclasite/gouge-filling, in the “hanging wall”. Thin fractures filled with calcite, reddish and greenish material, are penetrating the sandstone. Another sandstone-occurrence is found about one meter from the sampled occurrence.

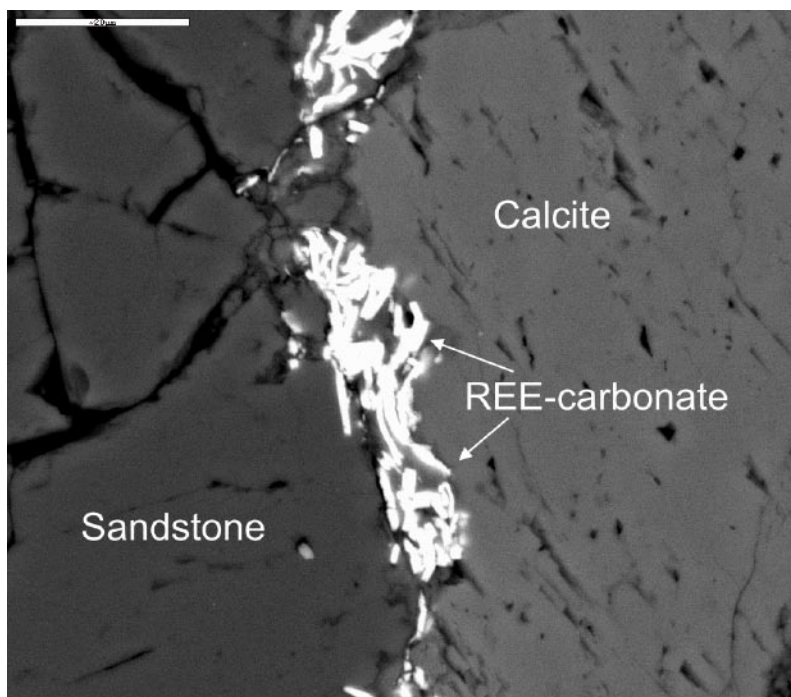
Minerals: Quartz, K-feldspar, chlorite, hematite, calcite, REE-carbonate, illite (possibly) and fluorite.

The sandstone consists of clasts of rounded quartz crystals and more fine-grained quartz crystals as cement. In places K-feldspar can be seen in the pore space between the quartz clasts. The sandstone is more or less made up of pure quartz crystals in its unaltered parts. The sandstone often shows increased alteration towards the cataclasite. This alteration is shown by longer distance between the clasts and appearance of other minerals, especially K-feldspar in the cement between the clasts. Other minerals in the cement of this altered part of the sandstone are chlorite and presumably illite. Small crystals of hematite may also be found in these parts.

The cataclasite consists of adularia and subordinate chlorite (Fe-rich) and hematite. The hematite content varies much within the cataclasite. This variation does not always coincide with the red coloration seen in hand sample and optical microscope. A large part of the cataclasite is made up of quartz and K-feldspar fragments. The K-feldspar fragments are thought to be from the wall rock while some the quartz fragments originate from the sandstone. The quartz clasts of sandstone origin in the cataclasite are distinguished from the quartz fragments from the wall rock in that they are rounded and unaltered. The cement in the altered part of the sandstone resembles the hematite-rich cataclasite in mineral composition but is less frequent in hematite.

Calcite (undetectable amount of MnO<sub>2</sub>) and fluorite fill a thin fracture that penetrates the sandstone, and the cataclasite. REE-carbonate, rich in La, Ce, Nd and Ca, coats the fracture wall of the calcite filling and is therefore thought to be coeval with calcite and fluorite.





*Back-scattered SEM-image of a fracture filled with calcite and REE-carbonate that cut through the sandstone. Scale marker bar is 20  $\mu$ m. From sample 271.53–271.63 m (I).*

### **KSH03A: 271.53–271.63 m (II)**

Sample type: Thin section.

Rock type: Sandstone.

Fracture: This thin section is prepared from the sandstone close to the thin section described above. In this thin section the sandstone dominates and a thin filling of greenish material with reddish parts penetrates the sandstone. The sandstone is bordered by reddish, cataclastic material in the outermost parts of the thin section.

Minerals: Quartz, K-feldspar, illite, albite, chlorite, hematite, Ti-oxide, zircon, apatite and small amounts of REE-carbonate.

The sandstone consists of clasts of rounded quartz crystals and more fine-grained quartz crystals as cement. In places K-feldspar can be seen in the pore space between the quartz clasts. The sandstone is more or less made up of purely quartz crystals in its unaltered parts. The sandstone often shows an increased alteration with decreased distance to the bordering hematite-cataclasite. This alteration is shown by increased distance between the clasts and increased amount of K-feldspar in the cement between the clasts. Zircon is also present in the sandstone.

The very fine-grained hematite-cataclasite consists of K-feldspar (Fe-stained adularia) and subordinate chlorite, albite, illite, hematite and additional crystals of apatite. A large part of the cataclasite is made up of quartz and K-feldspar fragments. The K-feldspar fragments are thought to be of wall rock origin while some the quartz fragments originate from the sandstone.

A green-coloured filling penetrates through the sandstone. The filling seems to “grow” from the hematite-cataclasite and into the sandstone. The filling consists of mainly K-feldspar (both as large subhedral crystals and as fine-grained crystals), illite (possibly in mixed layer-clay with chlorite) and subordinate Ti-oxide, albite, hematite, chlorite and fragments

of quartz and apatite. Ti-oxide seems to be the latest formed mineral in parts of the filling, and is occasionally found in association with illite and sporadic and very fine-grained crystals of REE-carbonate.

**KSH03A: 295.80–296.07 m**

Sample type: Thin section.

Rock type: Ävrö granite, medium oxidised.

Fracture: Networks of thin (< 5 mm) fine-grained fillings of two generations. The older is green-coloured and the younger is dark red to brown (e.g. 178/39°). Both of these fillings are cut by 2–7 mm wide fractures filled with dominantly calcite. The younger fillings seem to occupy re-activated fractures through the earlier formed fillings (e.g. 221/24°).

Minerals: Quartz, adularia, chlorite, hematite, epidote and albite.

Order of fracture fillings:

1. Epidote-rich cataclasite with subordinate crystals of albite and Fe-Mg-chlorite.
2. Hematite-cataclasite consisting of Mg-rich chlorite, adularia and hematite, in order of abundance.
3. Quartz-rich filling, occasionally containing Mg-rich chlorite, adularia, and hematite.
4. Fe-rich chlorite in micro-fractures cutting through quartz.

Wall rock alteration: Foliated and fine-grained wall rock with highly strained quartz-rich and epidote-rich sections. Some larger primary crystals of plagioclase, quartz and K-feldspar are still present. Pseudomorphs after primary plagioclase are red-stained.



*Photograph of drill core sample 295.80–296.07 m showing fractures filled with e.g. hematite, adularia, chlorite (red to brown) and quartz (bright). Drill core diameter is about 50 mm.*

**KSH03A: 305.64–305.76 m**

Sample type: Thin section.

Rock type: Ävrö granite, medium oxidized.

Fracture: Two fracture sets occur in this sample. The first is a breccia-like/cataclastic network of < 1 mm thin fractures that are irregularly distributed (e.g. 98/83° and 107/70°). There are two varieties of this filling, one green and one red coloured. An orthogonal fracture network, with mm-wide fillings of calcite, cuts this fracture network dominantly (176/48°).

Minerals: Calcite, quartz, adularia, hematite, albite, chlorite and epidote.

Order of fracture fillings:

1. Epidote-rich cataclasite, also consisting of adularia, quartz, albite, chlorite and minor amounts of hematite.
2. Hematite-cataclasite consisting of Mg-rich chlorite (MgO = 18%, FeO = 4%), Fe-rich chlorite (MgO = 12%, FeO = 35%), adularia, epidote, quartz and albite with titanite. Hematite is not very abundant but still gives the filling a dark red appearance.
3. A fracture filled with calcite (MnO<sub>2</sub> = n.d. to 0.1% with many fluid inclusions) and quartz is cutting through the hematite-cataclasite perpendicularly. Some hematite is present along with quartz.
4. Calcite (MnO<sub>2</sub> = 0.6–1.1%) with some Fe-rich chlorite (MgO = 6%, FeO = 36%), Mg-rich chlorite (MgO = 21%, FeO = 4%), adularia and hematite are filling fractures that reactivate the hematite-cataclasite. One of these fractures cuts through and offsets the calcite fracture (2). These later formed calcite filled fractures are much thinner than the fracture in “generation 2”. Hematite is present on the fracture walls of these fractures. Albite is present in voids of the calcite.

Wall rock alteration: Somewhat red-stained and foliated wall rock with high amount of micro-fractures. Quartz crystals are undulose and polycrystalline crystals are abundant. The primary plagioclase is completely replaced by e.g. albite, and K-feldspar, in a pseudomorphic manner. The pseudomorphs are red-stained. The primary microcline remains fresh.

#### ***KSH03A: 340.92–341.06 m***

Sample type: Thin section.

Rock type: Ävrö granite, weakly oxidized.

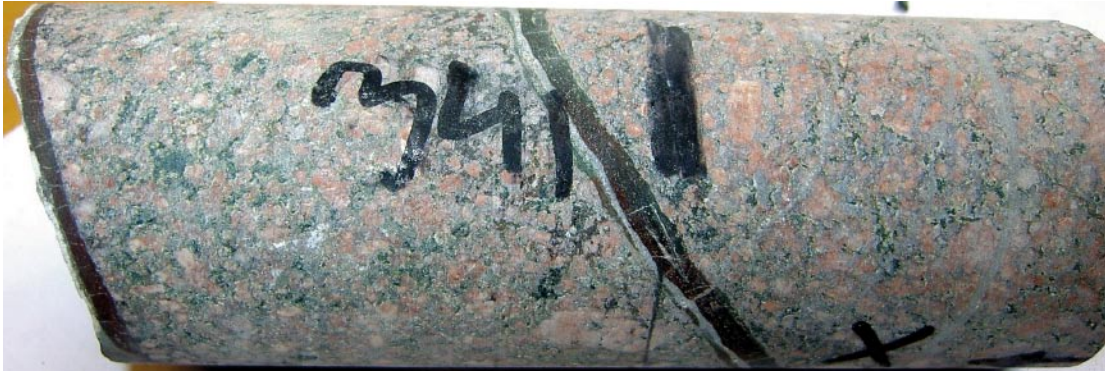
Fracture: 6 mm wide fracture filled with a 4 mm wide reddish brown filling and a 2 mm wide white to grey filling (241/68°). The latter was formed when the first filling was broken up by re-activation of the fracture.

Minerals: Quartz, adularia, chlorite, epidote and small amounts of illite (possibly).

Order of fracture fillings:

1. Cataclasite with matrix consisting of Mg-rich chlorite and adularia (and possibly also illite). Fragments consist of epidote and quartz. Some very fine-grained hematite crystals are present as well.
2. Thin quartz-dominated veins with associated adularia and some fragments of Mg-rich chlorite, are cutting through the cataclasite.

Wall rock alteration: Primary plagioclase is completely replaced by e.g. albite and K-feldspar, in a pseudomorphic manner. Primary plagioclase twinning is occasionally preserved in the pseudomorphs. The pseudomorphs after primary plagioclase are red-stained. Fine-grained, polycrystalline quartz is present in minor fractures, often along grain boundaries of primary crystals.



*Photograph of drill core sample 340.92–341.06 m showing a fracture filled with e.g. hematite, adularia and chlorite (red to brown) that is cut by a fracture filled with dominantly quartz and adularia (bright). Drill core diameter is about 50 mm.*

**KSH03A: 495.42 m**

Rock type: Fine-grained granite.

Fracture: Open fracture.

Minerals according to X-Ray Diffraction: Gypsum and fluorapophyllite.

**KSH03A: 684.46 m**

Rock type: Ävrö granite, weakly oxidized.

Fracture: Open fracture.

Minerals according to X-Ray Diffraction: Gypsum and natroapophyllite.

**KSH03A: 863.66–863.84 m**

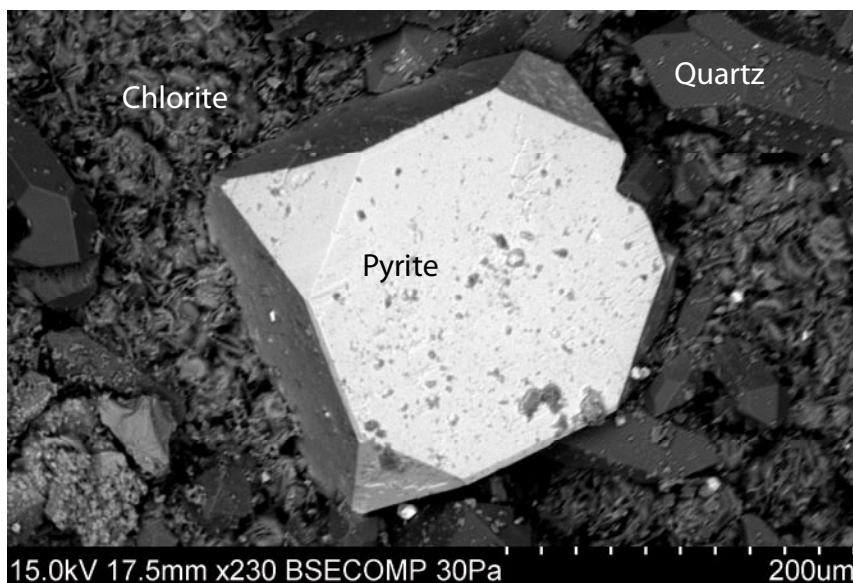
Sample type: Thin section.

Rock type: Mylonite affecting weakly oxidised granite.

Fracture: > 20 cm thick light green mylonite (lower rim 237/50°) including wall rock fragments. Two sets of thin (< 1 mm) fractures sealed with green and red coloured fillings are penetrating the mylonite. One of these sets (e.g. 301/74° and 320/77°) is dominant.

The mylonite matrix consists of about 80–90% of fine-grained epidote and the rest is K-feldspar and quartz. Angular fragments in the mylonite are from the wall rock.

The fractures cutting through the mylonite are filled with K-feldspar (red), quartz and chlorite (green). Most of the fractures are only filled with K-feldspar and quartz. When chlorite, K-feldspar and quartz appear in the same fracture, the chlorite is present in the centre of the fracture and K-feldspar and quartz coat the fracture. The chlorite is of Fe-Mg-type (FeO = 24–26%, MgO = 16–17%).



*Back-scattered SEM-image of a cubic pyrite crystal, euhedral quartz crystals and fine-grained chlorite crystals. From sample 863.66–863.84 m.*

### **KSH03A: 863.66–863.84 m**

Sample type: Surface sample.

Rock type: Mylonite affecting weakly oxidised granite.

Fracture: Open fracture.

Minerals: Calcite, pyrite, quartz, chlorite, barite and Cu-oxide.

Calcite (mostly scalenohedral) is present along with cubic pyrite crystals and euhedral quartz crystals on a Fe-rich chlorite coating. Small amounts of barite and Cu-oxide (Sn-rich) is also present on the fracture surface.

## **A2 SEM-EDS-analyses**

Detection limit of SEM-EDS is about 0.3% for Na<sub>2</sub>O and about 0.1% for other oxides. The SEM-EDS analyses give values of the total Fe-oxide content, distinctions of Fe<sup>2+</sup> and Fe<sup>3+</sup> can not be made. “n.d.” = below the detection limit.

<b>K-feldspar (Adularia)</b>	<b>Al<sub>2</sub>O<sub>3</sub></b>	<b>SiO<sub>2</sub></b>	<b>K<sub>2</sub>O</b>	<b>CaO</b>	<b>BaO</b>	<b>FeO</b>	<b>Total</b>
14.97–15.32(1)	18.71	65.34	16.24	n.d.	n.d.	0.45	100.74
126.00–126.22(1)	18.68	65.27	16.09	0.13	0.59	n.d.	100.73
863.66–863.84	18.68	64.05	16.64	n.d.	n.d.	n.d.	99.37

<b>Barite</b>	<b>Na<sub>2</sub>O</b>	<b>Al<sub>2</sub>O<sub>3</sub></b>	<b>SO<sub>3</sub></b>	<b>CaO</b>	<b>SrO</b>	<b>BaO</b>	<b>Total</b>
177.74–177.81-1	0.56	0.87	33.88	3.08	9.67	48.05	96.72
220.15–220.31	0.91	0.80	34.99	0.81	n.d.	63.88	101.39

<b>Epidote</b>	<b>Al<sub>2</sub>O<sub>3</sub></b>	<b>SiO<sub>2</sub></b>	<b>CaO</b>	<b>MnO</b>	<b>FeO</b>	<b>Total</b>
863.66–863.84(1)*	22.85	37.81	22.59	n.d.	12.77	96.02
863.66–863.84(2)*	24.04	37.67	23.01	n.d.	11.59	96.31
863.66–863.84(3)*	23.63	37.46	22.73	0.18	11.49	95.49

<b>Illite</b>	<b>MgO</b>	<b>Al<sub>2</sub>O<sub>3</sub></b>	<b>SiO<sub>2</sub></b>	<b>K<sub>2</sub>O</b>	<b>CaO</b>	<b>FeO</b>	<b>Total</b>
126.00–126.22-1	5.30	21.80	53.40	6.75	0.50	2.54	90.29
186.52–186.62*	4.99	23.06	48.40	6.51	0.47	6.02	89.91
220.15–220.31(1)	4.48	22.81	53.59	6.72	0.63	4.07	92.30
220.15–220.31(2)	4.26	22.04	52.29	6.57	0.62	3.07	88.87
220.15–220.31(3)	5.02	23.04	54.43	6.87	0.61	4.73	94.70
220.15–220.31(4)	3.85	21.83	55.11	7.61	0.65	3.34	92.39
245.03–245.07(1)	5.10	22.74	50.95	6.34	n.d.	2.98	88.11
245.03–245.07(2)	4.28	22.70	52.72	7.08	n.d.	3.56	90.34
245.03–245.07(3)	4.53	22.43	52.27	6.29	0.61	2.17	88.28

\* = incl. 0.47 Na<sub>2</sub>O.

<b>Fe-Mg-chlorite</b>	<b>MgO</b>	<b>Al<sub>2</sub>O<sub>3</sub></b>	<b>SiO<sub>2</sub></b>	<b>MnO</b>	<b>FeO</b>	<b>Total</b>
863.66–863.84(1)	15.85	16.38	28.11	0.52	26.33	87.19
863.66–863.84(2)	16.56	16.22	29.13	0.42	23.96	86.29

<b>Mg-chlorite</b>	<b>MgO</b>	<b>Al<sub>2</sub>O<sub>3</sub></b>	<b>SiO<sub>2</sub></b>	<b>K<sub>2</sub>O</b>	<b>CaO</b>	<b>TiO<sub>2</sub></b>	<b>MnO</b>	<b>FeO</b>	<b>Total</b>
111.80–111.92-1	18.41	18.13	36.45	1.11	0.96	0.13	0.54	9.30	85.01
111.80–111.92-2	15.33	19.18	36.31	0.77	3.69	0.40	0.61	9.01	85.29
220.15–220.31-1	15.60	21.30	40.22	1.80	0.40	n.d.	0.17	5.99	88.53
225.44–225.49-1	15.63	19.48	37.13	1.60	0.97	0.56	0.25	9.82	85.44
225.44–225.49-2	14.88	20.34	41.30	2.70	0.48	n.d.	0.16	7.70	87.57
295.80–296.07-1	16.22	23.91	38.84	0.77	0.80	0.23	0.35	6.06	87.17
295.80–296.07-2	16.12	24.11	38.43	0.62	0.87	0.21	0.30	7.90	88.55

Fe-chlorite	Na <sub>2</sub> O	MgO	Al <sub>2</sub> O <sub>3</sub>	SiO <sub>2</sub>	K <sub>2</sub> O	CaO	TiO <sub>2</sub>	MnO	FeO	Total
126.00–126.22(2)-1	0.33	6.27	14.57	26.99	0.38	0.31	n.d.	0.52	37.15	86.52
126.00–126.22(2)-2	n.d.	4.53	15.95	26.62	1.00	0.32	n.d.	0.36	35.23	84.02
126.00–126.22(2)-3	n.d.	6.36	16.12	29.69	0.41	0.41	n.d.	0.43	35.32	88.75
126.00–126.22(2)-4	n.d.	6.60	15.01	27.65	0.32	0.36	n.d.	0.40	37.00	87.35
220.15–220.31-1	n.d.	2.98	12.37	26.31	0.13	0.58	n.d.	0.20	42.80	85.37
220.15–220.31-2	0.33	3.14	12.77	27.05	0.42	0.52	n.d.	0.00	42.14	86.38
220.15–220.31-3*	n.d.	3.02	11.95	25.20	n.d.	2.84	n.d.	0.16	40.40	83.56
233.56–233.67-1*	0.57	3.17	7.75	23.58	0.63	0.98	0.18	n.d.	41.72	78.58
233.56–233.67-2*	0.32	4.75	8.86	31.69	0.26	0.67	n.d.	0.14	40.46	87.15
233.56–233.67-3*	0.43	4.85	8.78	30.66	0.15	1.36	n.d.	n.d.	32.64	78.87
233.56–233.67-4*	0.41	4.51	8.98	30.51	0.44	0.89	n.d.	n.d.	31.01	76.74
233.56–233.67-5*	0.58	4.37	8.71	28.40	0.50	0.92	n.d.	n.d.	36.03	79.50
233.56–233.67-6**	n.d.	2.94	8.10	22.62	n.d.	0.66	n.d.	n.d.	46.13	81.10
233.56–233.67-7*	n.d.	4.60	9.07	31.90	0.13	1.19	n.d.	n.d.	41.76	88.65
245.03–245.07*	0.43	9.72	14.28	26.12	1.02	2.20	1.64	0.33	33.54	89.28

" = incl. 0.63 V<sub>2</sub>O<sub>5</sub>.

\* = probably in ML with clay minerals (corrensite).

Laumontite	Na <sub>2</sub> O	Al <sub>2</sub> O <sub>3</sub>	SiO <sub>2</sub>	K <sub>2</sub> O	CaO	Total
126.00–126.22-2(1)	0.24	22.35	54.01	0.64	10.76	87.99
126.00–126.22-2(2)	0.38	22.04	53.96	0.64	10.55	87.57

Prenhite	Al <sub>2</sub> O <sub>3</sub>	SiO <sub>2</sub>	CaO	FeO	Total
126.00–126.22-2	21.84	43.59	26.78	3.36	95.57

### A3 X-Ray Diffraction results

The table only shows occurrence of different minerals in the samples, no relative abundance is shown.

Depth(m)	Quartz	Micro-cline	Musco-vite	Calcite	Chlorite	Laumon-tite	Antigo-rite	Hematite	Gypsum	Apop-hyllite	Clay mineral in addition to chlorite
14.97–15.32(l)	x	x		x	x						(x)illite
117.75–117.94	x	x		x	x			x			x corrensite
159.69						x					
180.03	x		x	x			x				
181.93–181.98						x					
495.42									x	x <sup>1</sup>	
684.46									x	x <sup>2</sup>	

Corrensite = (Mg,Al)<sub>3</sub>(Si,Al)<sub>8</sub>O<sub>20</sub>(OH)<sub>10</sub>\*4H<sub>2</sub>O = swelling mixed layer clay with chlorite/smectite or chlorite/vermiculite regularly interlayered.

Antigorite = Mg<sub>3</sub>Si<sub>2</sub>O<sub>5</sub>(OH)<sub>4</sub>.

<sup>1</sup> = Fluorapophyllite = KCa<sub>4</sub>(Si<sub>4</sub>O<sub>20</sub>)F\*8H<sub>2</sub>O.

<sup>2</sup> = Natroapophyllite = NaCa<sub>4</sub>Si<sub>6</sub>O<sub>20</sub>F\*8H<sub>2</sub>O.

## A4 Stable isotopes

### Isotope analyses of calcite ( $\delta^{13}\text{C}$ , $\delta^{18}\text{O}$ , $^{87}\text{Sr}/^{86}\text{Sr}$ ).

Sample	$\delta^{13}\text{C}$ (‰)	±	$\delta^{18}\text{O}$ (‰)	±	$^{87}\text{Sr}/^{86}\text{Sr}$	±
KSH03 – 14.97–15.32	-10.357	0.1	-14.132	0.1		
KSH03 – 111.80–111.92	-4.181	0.1	-13.621	0.1	0.710657	0.000013
KSH03 – 117.75–117.94	-6.178	0.1	-19.843	0.1		
KSH03 – 126.00–126.22-2	-13.984	0.1	-9.43	0.1		
KSH03 – 177.74–177.81-1	-3.124	0.1	-19.512	0.1	0.707183	0.000016
KSH03 – 177.74–177.81-2	-3.917	0.1	-21.77	0.1		
KSH03 – 181.93–181.98(1)	-3.028	0.1	-16.998	0.1	0.707497	0.000015
KSH03 – 181.93–181.98(2)	-3.55	0.1	-16.089	0.1		
KSH03 – 186.52–186.62	-13.853	0.1	-13.504	0.1		
KSH03 – 197.79–197.85	-5.02	0.1	-17.486	0.1		
KSH03 – 220.15–220.31	-9.463	0.1	-11.264	0.1	0.712188	0.000030
KSH03 – 225.44–225.49	-12.289	0.1	-12.594	0.1	0.722189	0.000026
KSH03 – 305.64–305.76(1)	-3.891	0.1	-21.627	0.1		
KSH03 – 305.64–305.76(2)	-5.988	0.1	-14.215	0.1		
KSH03 – 863.66–863.84	-21.166	0.1	-12.152	0.1	0.715368	0.000025